TECHNICAL INFORMATION RELEASE

management and technical services company

TIR 2114-MED-5010

FROM	**TO**		
Alan W. Nordheim	N. Cintron, Ph.D./SD4		
DATE	**CONTRACT NO:**	**T.O. OR A.D. REF:**	**MIS OR OTHER NASA REF:**
May 1985	NAS9-17151		

SUBJECT A Detailed Analysis of the Erythropoietic Control System in the Human, Squirrel Monkey, Rat and Mouse

This report provides a detailed description of the erythropoiesis modeling performed in support of the Body Fluid and Blood Volume Regulation tasks under Contract NAS9-17151. This report includes a description of the mathematical formulation of the species-independent model, the solutions to the steady-state and dynamic versions of the model, as well as the individual species-specific models for the human, squirrel monkey, rat and mouse. The analysis portion of this report is composed of two parts. The first part is a detailed sensitivity analysis of the species-independent model response to parameter changes and how those responses change from species-to-species. The second part of the study is an analysis of the species-to-species response to a series of simulated stresses directly related to blood volume regulation during space flight.

Alan W. Nordheim

Alan W. Nordheim

/db

Attachment

Unit Manager

Approving NASA Manager F.A. Kutyna, Ph.D. **Concurrence**

DISTRIBUTION

NASA/HQS: R. J. White

MATSCO/HQS: L. Griffiths

NASA/JSC:
BE3/B.J. Jefferson
SA/W. H. Shumate
SB/J. Vanderploeg
SD2/J. Logan
SD3/M. Bungo
/J. Charles
/P. Johnson
/V. Schneider

MATSCO/HO:
R. F. Meyer
Mission Sci.Group
TIR Files

GE/HO:
T.D. Gregory(2)
Contracts File

2114-MED-5010

A DETAILED ANALYSIS OF THE ERYTHROPOIETIC CONTROL SYSTEM IN THE HUMAN, SQUIRREL MONKEY, RAT AND MOUSE

Prepared by

Alan W. Nordheim
Biomedical Research Engineer

Management and Technical Services Company
Houston, Texas

Contract NAS9-17151

April 1985

A DETAILED ANALYSIS OF THE ERYTHROPOIETIC CONTROL SYSTEM IN THE HUMAN, SQUIRREL MONKEY, RAT AND MOUSE

Alan W. Nordheim
Management and Technical Services Company
Houston, Texas

April 1985

Abstract

This report provides a detailed description of the erythropoiesis modeling performed in support of the Body Fluid and Blood Volume Regulation Tasks under contract NAS9-17151. This report includes a description of the mathematical formulation of the species independent model, the solutions to the steady-state and dynamic versions of the model, as well as the individual species-specific models for the human, squirrel monkey, rat, and mouse. The analysis portion of this report is composed of two parts. The first part is a detailed sensitivity analysis of the species-independent model response to parameter changes and how those responses change from species-to-species. The second part of the study is an analysis of the species-to-species response to a series of simulated stresses directly related to blood volume regulation during space flight.

TABLE OF CONTENTS

No.	Title	Page
1.0	INTRODUCTION	1
2.0	SPECIES-INDEPENDENT MODEL OF ERYTHROPOIESIS	2
2.1	PHYSIOLOGICAL BASIS OF THE GENERAL MODEL OF ERYTHROPOIESIS	2
2.1.1	Description of Species-Independent Model	4
2.1.2	Steady-State Solution	10
2.1.3	Dynamic Solution	11
2.2	SPECIES-SPECIFIC MODELS	12
2.2.1	Validation Simulations	12
2.2.1.1	Human Model Revalidation	13
2.2.1.2	Squirrel Monkey Model Validation	14
2.2.1.3	Rat Model Validation	17
2.2.1.4	Mouse Model Validation	17
2.2.2	Discussion on Model Validations	19
3.0	SPECIES COMPARISON	22
3.1	SENSITIVITY ANALYSIS	22
3.1.1	Steady-State Sensitivity Analysis	22
3.1.1.1	Parameter Variation	22
3.1.1.2	Parameter Sensitivities	31
3.1.1.3	Discussion on Steady-State Sensitivities	40
3.1.2	Dynamic Sensitivity Analysis	48
3.2	SIMULATED STRESSES	56
3.2.1	Long-Term Hypoxic Exposure and Recovery	58
3.2.2	Red Cell Infusion/Red Cell Loss	60
3.2.3	Erythropoietin Infusion	63
3.2.4	Plasma Volume Depletion	64

TABLE OF CONTENTS (Continued)

No.	Title	Page
4.0	DISCUSSION	69
5.0	REFERENCES	71
APPENDIX A	. . . . .	A-1
APPENDIX B	. . . . .	B-1

1.0 INTRODUCTION

New experimental studies of body fluid and blood volume regulation (including studies of erythropoiesis regulation) during space flight and in terrestrial surroundings are being considered which utilize, not only human subjects, but animals such as the laboratory mouse, rat, and monkey. Mathematical models representing the human and murine erythropoietic systems have been previously developed (1,2), and have been useful in elucidating the mechanisms involved in the control of erythropoiesis and, therefore, blood volume regulation, under a variety of stress situations, including space flight. In order to better understand previous space-flight results, and to help analyze the data from these new multi-species experiments, and to help relate experimental results among species, a uniform, species-independent, modeling approach to the erythropoiesis system has been developed. This approach allows the problem of species variation to be addressed by design. This report is a summary of the results from a series of simulation studies using the species independent model to compare the erythropoietic control systems in the human, squirrel monkey, rat, and mouse. The report includes a description of the mathematical formulation of the species-independent model, the steady-state and dynamic solutions of the model, and the validation simulations for all four species models. The report also includes a detailed analysis of erythropoiesis control and its relation to blood volume regulation. The first part of the analysis consists of a discussion of the steady-state and dynamic sensitivity analysis which was performed to study how the basic model of erythropoiesis responds to changes in parameters and how these responses differ between the four species. The second part of the analysis is a discussion of the species-to-species response to a series of simulated stresses that are directly related to blood volume regulation during space flight.

2.0 SPECIES-INDEPENDENT MODEL OF ERYTHROPOIESIS

This section of the report is a summary of the physiological concepts used in the development of the original model of erythropoiesis, the development of the species-independent model of erythropoiesis model, the steady-state model solution, the dynamic model solution, and the validations of the species-specific model.

The problem of developing species specific models was approached in the following manner. The equations from the original model of erythropoiesis (1) were rederived to produce a minimal set of equation and parameters (3,4). In its mathematically reduced form, the model consists of three non-linear differential equations and contains twelve parameters. The differential equations have been scaled using the normal values of the three dependent variables (red cell mass, plasma concentration of erythropoietin, and red blood cell production rate). The twelve independent parameters are determined from the original model and are each a composite of several physiological parameters. The physiological parameter values themselves are dependent upon the species of interest. Reducing the number of parameters and equations in this manner simplifies the analysis of the functioning of the model, since the model can be studied in this more generalized form. This new formulation of the model is ideal for studying interspecies variations, for once it is understood how the model functions in general, the aspect of species variation can be studied simply by changing the physiological parameter values, while the overall model structure remains the same.

2.1 PHYSIOLOGICAL BASIS OF THE GENERAL MODEL OF ERYTHROPOIESIS

The original erythropoiesis model (1) was developed to study the relative influence of the controlling factors of erythropoiesis on total red cell mass. Those elements of importance to the feedback regulation of erythropoiesis that have been incorporated into the model are shown in Figure 1. This formulation was based on the concept that the overall balance between oxygen supply and demand regulates the release of the hormone erythropoietin from renal tissues sensitive to oxygen tension levels and which, in turn, controls bone marrow red cell production.

FIGURE 1. SYSTEMS DIAGRAM OF THE MAJOR PHYSIOLOGICAL ELEMENTS IN THE ERYTHROPOIESIS CONTROL MODEL
(Leonard, et.al. 1981)

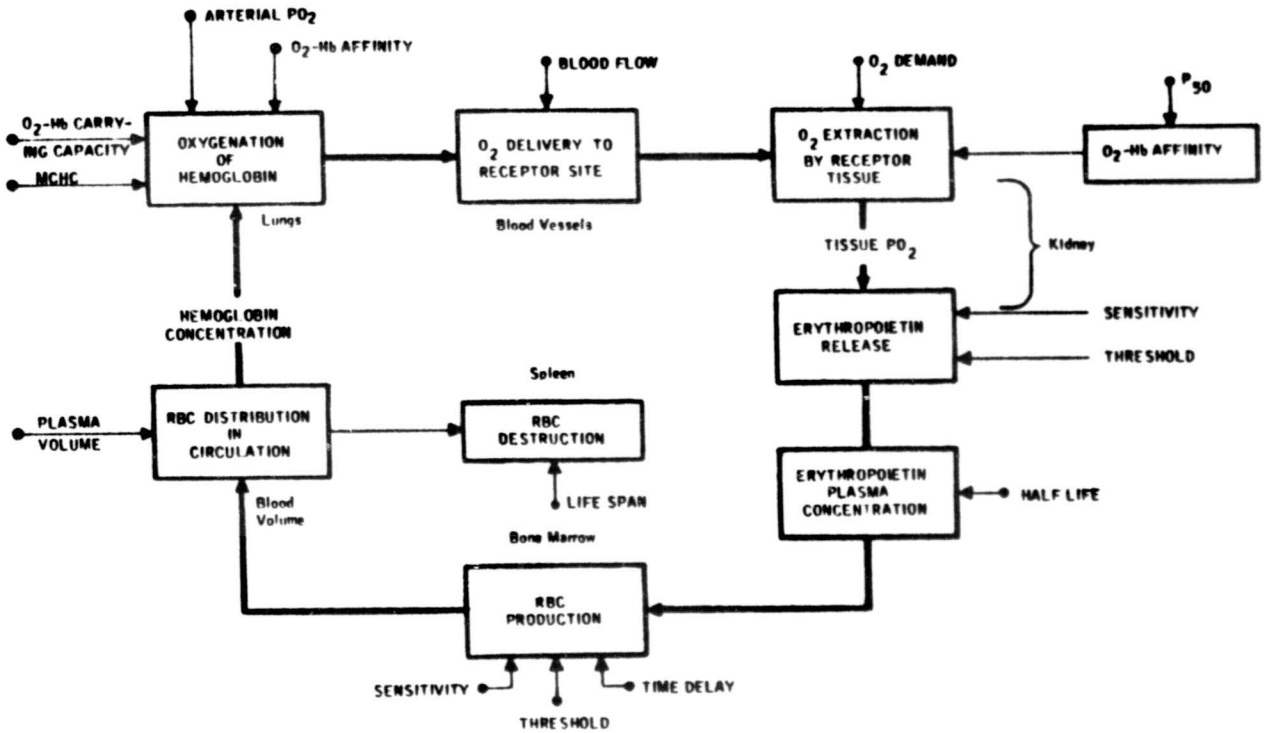

Renal oxygen tissue tension is influenced by several factors: hemoglobin concentration, lung oxygenation of hemoglobin, renal blood flow, and oxygen-hemoglobin affinity. A fraction of the oxygen reaching the kidney is extracted by the tissues depending on the oxygen demand parameter. Oxygen enters the renal tissue by diffusion along an oxygen gradient between the venous capillaries and the tissue cells. A decrease in the oxygen supply in relation to the oxygen demand will reduce the tissue oxygen tension and result in an increased rate of erythropoietin release. Erythropoietin is released into general circulation with the plasma concentration being determined by the rate of release, volume of distribution, and the rate at which it is metabolized. The target of erythropoietin is the hemopoietic tissue. The production rate and release of red cells are determined by the plasma concentration of erythropoietin. There is a time delay between marrow stimulation and red cell release. The rate of red blood cell destruction is based on the life span of the cell and is assumed to be a fixed percentage of the red cell mass.

The physiological derivations of the original model equations, upon which the following work is based, can be found in reference (1).

2.1.1 Description of Species-Independent Model

The structure of the model is relatively simple, but non-linear. The original model can be reduced to the following three non-linear differential equations containing twelve "mathematical" parameters (that is, parameters which have no direct physiological meaning, but are composed of several physiological parameters).

$$\dot{x} = K_1 (z - x) \quad , \quad x(o) = 1 \tag{1}$$

$$\dot{y} = K_2 (F_2(x) - y) \quad , \quad y(o) = 1 \tag{2}$$

and

$$\dot{z} = K_3 \, (F_3(y) - z) \, , \quad y(o) = 1 \tag{3}$$

In these equations, the $\dot{x}$ represents the time derivative dx/dt. The non-linear functions $F_2(x)$ and $F_3(y)$ are defined as follows:

$$F_2(x) = A \exp\left\{ - B \left[\frac{Cx-1}{Dx+1} \right]^n \right\} \tag{4}$$

and

and

$$F_3(y) = \begin{cases} y^{G_2} & , \; y < 1 \\ 1 + G_2 \log y & , \; 1 \leq y \leq e^{4/G_2} \\ 6 - \exp\left\{ G_2 (1 - y \; e^{-4/G_2}) \right. & , \; e^{4/G_2} < y \end{cases} \tag{5}$$

Variables and parameters for this model are defined below and in Table 1. The dependent variables x, y, and z represent normalized values of red cell mass, erythropoietin level in the blood, and red cell production rate. The mathematical parameters utilized in equations 1-5 are defined as follows in terms of the physiological parameters.

$$K_1 = \log 2 \; / \; TRC_{\frac{1}{2}} \; , \tag{6}$$

$$K_2 = \log 2 \; / \; TE_{\frac{1}{2}} \; , \tag{7}$$

$$K_3 = 1 \; / \; TBM \; , \tag{8}$$

$$A = \exp\left\{ G_1 \left(1 + \frac{V_m}{K_d \cdot P_t O_o} \right) \right\} \; , \tag{9}$$

Table 1. Definition of Primary Model Parameters

Symbol	Definition
CHbU	Carrying capacity of hemoglobin
E	Erythropoietin plasma concentration
E_o	Normal Erythropoietin plasma concentration
G_1	Gain of renal erythropoietin production control function
G_2	Gain of marrow RCP control function
k	Exponent in the Hill equation describing oxygen-hemoglobin equilibrium
k_d	Capillary diffusivity
MCHC	Mean corpuscular hemoglobin concentration
P_{50}	Oxygen tension of blood at 50 percent hemoglobin saturation
P_aO	Oxygen tension in arterial blood
P_tO_o	Normal value of oxygen tension in renal tissue fluid
PV	Plasma volume
Q	Renal blood flow
RCM	Red Cell Mass
RCM_o	Normal value of Red Cell Mass
RCP	Production rate of new red blood cells
RCP_o	Normal value of RCP
S_aO	Saturation of arterial hemoglobin with oxygen
TBM	Bone marrow transit time
$TE_{1/2}$	Plasma half-life of erythropoietin
$TRC_{1/2}$	Red cell half-life
V_m	Oxygen uptake of kidneys
x	Normalized red cell mass
y	Normalized erythropoietin concentration
z	Normalized red cell production

$$B = \frac{G_1 \cdot P_{50}}{P_t O_o} \quad , \tag{10}$$

$$C = \frac{Q \cdot MCHC \cdot CHbO \cdot S_a O - V_m}{V_m \cdot \frac{PV}{RCM_o}} \quad , \tag{11}$$

$$D = \frac{Q \cdot MCHC \cdot CHbO \cdot (1 - S_a O) + V_m}{V_m \cdot \frac{PV}{RCM_o}} \quad , \tag{12}$$

$$S_a O = \frac{1}{1 + \left(\frac{P_{50}}{P_a O}\right)^k} \quad , \tag{13}$$

and

$$n = 1/k \tag{14}$$

Note that the red cell mass (RCM), erythropoietin level (E), and red cell production rate (RCP) are related to x, y, and z as follows:

$$RCM = RCM_o \cdot x \tag{15}$$

$$E = E_o \cdot y \tag{16}$$

and

$$RCP = RCP_o \cdot z = K_1 RCM_o \cdot z \tag{17}$$

The values of the physiological parameters can be found in Table 2. The values of the mathematical parameters, as calculated using the physiological parameter values from Table are presented in Table 3. The rationale used for selecting these values, as well as the source of the values has been

Table 2. System Parameters for Erythropoiesis Control Model For Four Species: Man, Squirrel Monkey, Rat (Sprague-Dawley), and Mouse

Symbol	Units	Human	Squirrel Monkey	Rat (Sprague-Dawley)	Mouse
CHbO	ml O_2/g Hb	1.340	1.300 C	1.704 C	1.410
E_o	x normal	1.000	1.000	1.000 C	1.000
G_1	Non-dimensional	3.000	3.000 E	3.000 E	3.000
G_2	Non-dimensional	4.000	2.000 E	2.000 E	2.000
k	Non-dimensional	2.916	2.916 E	2.916 E	2.916
k_d	ml O_2/min mmHg	0.5663	0.2464 C	.0046 C	1.031×10^{-3}
MCHC	g Hb/ml RBC	0.3750	0.3220 A	.3340 A	.3000
P_{50}	mmHg	26.73	35.60 A	37.50 A	39.00
P_aO	mmHg	95.00	85.20	80.40	78.00
$P_{t\,o}$	mmHg	20.00	20.00 E	20.00 E	20.00
PV	ℓ	3.000	1.910×10^{-2}	5.600×10^{-2} A	7.700×10^{-4}
Q	ml/min	1200.	19.00 E	12.00 E	1.830
RCM_o	ℓ	2.000	1.390 x 10-2 A	4.400×10^{-3} A	6.300×10^{-4}
RCP_o	ℓ/min	1.528×10^{-5}	1.189×10^{-7} C	5.658×10^{-8} C	1.516×10^{-8}
TBM	min	5760.	3312.	5040. E	5040.0
$TE_{\frac{1}{2}}$	min	720.0	240.0 E	150.0	195.0
$TRC_{\frac{1}{2}}$	min	90720.	58460. E	38880. A	28800.0
V_m	ml O_2/min	20.00	.7200 C	.206 C	4.000×10^{-2}

A - Average reported values
C - Calculated from other physiological data
E - Estimated

Table 3. Mathematical Parameters for the Erythropoiesis Model for Each Species

Symbol	Definition	Human	Squirrel Monkey	Rat	Mouse
A	$\text{EXP}\ G_1\left(1 + \frac{V_m}{K_d \cdot P_{t}O_0}\right)$	4013.	1372.	1768.	6785
B	$\frac{G_1 \cdot P_{50}}{P_{t}O_0}$	4.010	5.340	5.625	5.850
C	$\frac{Q\ MCHC \cdot CHbO\ \ S_aO - V_m}{V_m \cdot \frac{PV}{RCM_0}}$	18.95	6.456	22.72	13.16
D	$\frac{Q\ MCHC \cdot CHbO \cdot (1 - S_aO) + V_m}{V_m \cdot \frac{PV}{RCM_0}}$	1.153	1.260	3.328	2.671
n	$1/K$	0.3429	0.3429	0.3429	0.3429
G_2	Gain of Marrow RCP Control Function	4.000	2.000	2.000	2.000
K_1	$\frac{\text{Log } 2}{TRC_{\frac{1}{2}}}$	7.641×10^{-6}	1.185×10^{-5}	1.783×10^{-5}	2.407×10^{-5}
K_2	$\frac{\text{Log } 2}{TE_{\frac{1}{2}}}$	9.627×10^{-4}	2.888×10^{-3}	4.621×10^{-3}	3.586×10^{-4}
K_3	$\frac{1}{TBM}$	1.736×10^{-4}	3.019×10^{-4}	1.984×10^{-4}	1.984×10^{-4}
S_aO	$\frac{1}{1 + \left(\frac{P_{50}}{P_aO}\right)^K}$	97.58	92.72	91.20	88.30

documented and can be found in TIR 2114-MED-2010 "System Parameters For the Species-Independent Model of Erythropoiesis Control: A Species Comparison of Normal Values in the Human, Squirrel Monkey, Rat, and Mouse Models."

Equations (1-3) can be solved numerically to generate either dynamic (time-dependent) solutions or steady-state (time-independent) solutions.

2.1.2 Steady-State Solution

The usual steady-state condition ($\dot{x} = \dot{y} = \dot{z} = 0$) leads to the non-liner equations

$$x = z \quad , \tag{18}$$

$$y = F_2(x) \quad , \tag{19}$$

and

$$z = F_3(y) \tag{20}$$

where $F_2(x)$ and $F_3(y)$ are defined by equations (4) and (5). Thus, at the steady-state

$$x = F_3(F_2(x)) \quad , \tag{21}$$

$$y = F_2(x) \quad , \tag{22}$$

and

$$z = x \quad . \tag{23}$$

Equation (21) can be solved by searching for the roots of the function

$$f(x) = x - F_3(F_2(x)). \tag{24}$$

Then, the desired value of x is the value for which $f(x) = 0$. This equation was solved numerically using a Newton-Raphson method. Once x is known, the steady-state values of y and z are obtained from equations (22) and (23).

2.1.3 Dynamic Solution

While the steady-state solution is easy to determine and is of interest to certain stress applications, often one wants or needs to know how the solution to these model equations change as a function of time. Equations (1-3) can be solved numerically to yield dynamic (i.e., time-dependent) solutions. The use of ordinary numerical integration techniques to solve these equations requires that a very small integration time step be used (less than one minute) in order to obtain accurate solutions. This is due to the fact that these equations represent a system of "stiff" differential equations. That is, the time constants associated with each equation (K_1, K_2, and K_3) differ from each other by orders of magnitude (see Table 3), a common occurrence in the modeling of many biological systems. Therefore, the hybrid Euler integration technique, which was developed for use in the original model of erythropoiesis (6,7), was used to solve for the time-dependent solution of the reformulated version of the erythropoiesis model. The hybrid Euler technique allows the integration step size to be increased from less than one minute to over 60 minutes without forfeiting solution accuracy. This increase in step size allows for the rapid numerical solution of the time-dependent equations for X, Y, and Z. The solutions to these equations can be converted to absolute values or used to calculate other hemopoietic indices and values that are based on these three variables (see references 1 and 4).

2.2 SPECIES-SPECIFIC MODELS

The formulation of the model, as described above, is not dependent on any species. The species influence only enters into the model through the mathematical parameters, which, in turn, are a function of certain physiological parameters. It is through these physiological parameters that species-specific aspects enter into the model. Therefore, to develop a species-specific model of erythropoiesis from the species independent model, the only step necessary is to collect the species specific parameter values that are necessary to calculate the mathematical parameters. Therefore, each species uses the same model formulation, but has a separate set of species-specific parameter values. The parameter values necessary for the human and mouse model were available from the two original models (1,2). However, in order to implement the rat and monkey models of erythropoiesis, an extensive literature search was performed to collect the necessary physiological data. Data were collected for the Sprague-Dawley rat and the squirrel monkey (Macaca Samiri) since these are the two species that are scheduled to be used as specimens onboard the Spacelab-4 dedicated Life Sciences Shuttle mission (including two hematology experiments). A description of the model reformulation, as well as the equations and parameters used in the model can be found in the TIR entitled "Analysis of a Twelve Parameter Nonlinear Model of Erythropoiesis" (3). The actual parameter values used for each model, along with the rationale for the selection of those values, has been documented and can be found in the TIR "System Parameters for the Species-Independent Model of Erythropoiesis Control: A Species Comparison of Normal Values in the Human, Squirrel Monkey, Rat, and Mouse Models" (4).

2.2.1 Validation Simulations

In order to verify that the reformulation of the human and mouse models produced results identical to the original models and to validate the squirrel monkey and rat models of erythropoiesis, all four models were validated/revalidated against experimental data that were not used to develop the models (i.e., not used to establish the species-specific data sets for each animal). Simulations of hypoxia, based upon actual experiments, were

performed using each of the four species models of erythropoiesis. The results of the simulations were compared with the experimental findings in order to verify the fact that the models compare both quantitatively, with respect to red cell mass, and qualitatively, with respect to red cell production and erythropoietin concentrations, associated with other typical hypoxia experiments. This combination of quantitative vs. qualitative comparison of results was necessary since there are few, if any, experiments which have studied all three of the model variables over periods of both hypoxic stress and recovery from hypoxic stress.

2.2.1.1 Human Model Revalidation. The human model was revalidated using the experimental data set used to validate the original erythropoiesis model (1). Buderer and Pace (8) studied the dynamic changes in red cell mass, hematocrit, and plasma volume in sea-level pig-tailed monkeys during and after a 6-month exposure to 3800 m altitude. Since comparable data for humans were not available, the experimental data were scaled to represent changes from normal. The original human model of erythropoiesis was validated using the same set of experimental data (3); therefore, a simulation of this experiment was performed in order to provide a verification of the model reformulation (see figure 2). This simulation was performed by changing arterial oxygen tension (P_aO) in a step fashion from 95 (normal P_aO at sea level) to 50 mmHg (P_aO at an altitude of 3800 m). This value of P_aO was selected from human altitude experimentation (9,10,11). The normalized red cell mass response of the model was adjusted by changing the bone marrow controller gain until agreement the simulation response was in agreement with the experimental red cell mass data. The model is also capable of predicting other variables that were not measured such as normalized plasma erythropoietin concentration and normalized red cell destruction rate as well as other hematological parameters that can be derived from these three variables.

The simulation shown in Figure 2 shows the squence of events that are assumed to generally characterize the hematological response to hypoxic stress, including reduced tissue oxygen tension (not shown), elevated erythropoietin concentration, and increased red cell production levels, all of which promote

FIGURE 2. Validation of Human Model of Erythropoiesis using a simulation of Altitude Hypoxia. The Validation simulation was based upon an experiment by Buderer and Nace (6) on pig-tailed Macaca Monkeys. The simulation of Hypoxia was performed by reducing PAO from 95 to 50 MMHG and G from 6.0 to 2.2. The recovery portion of the simulation was performed by returning PAO to normal and changing G to 12.0. All results have been normalized to a pre-stressed level of 1.0.

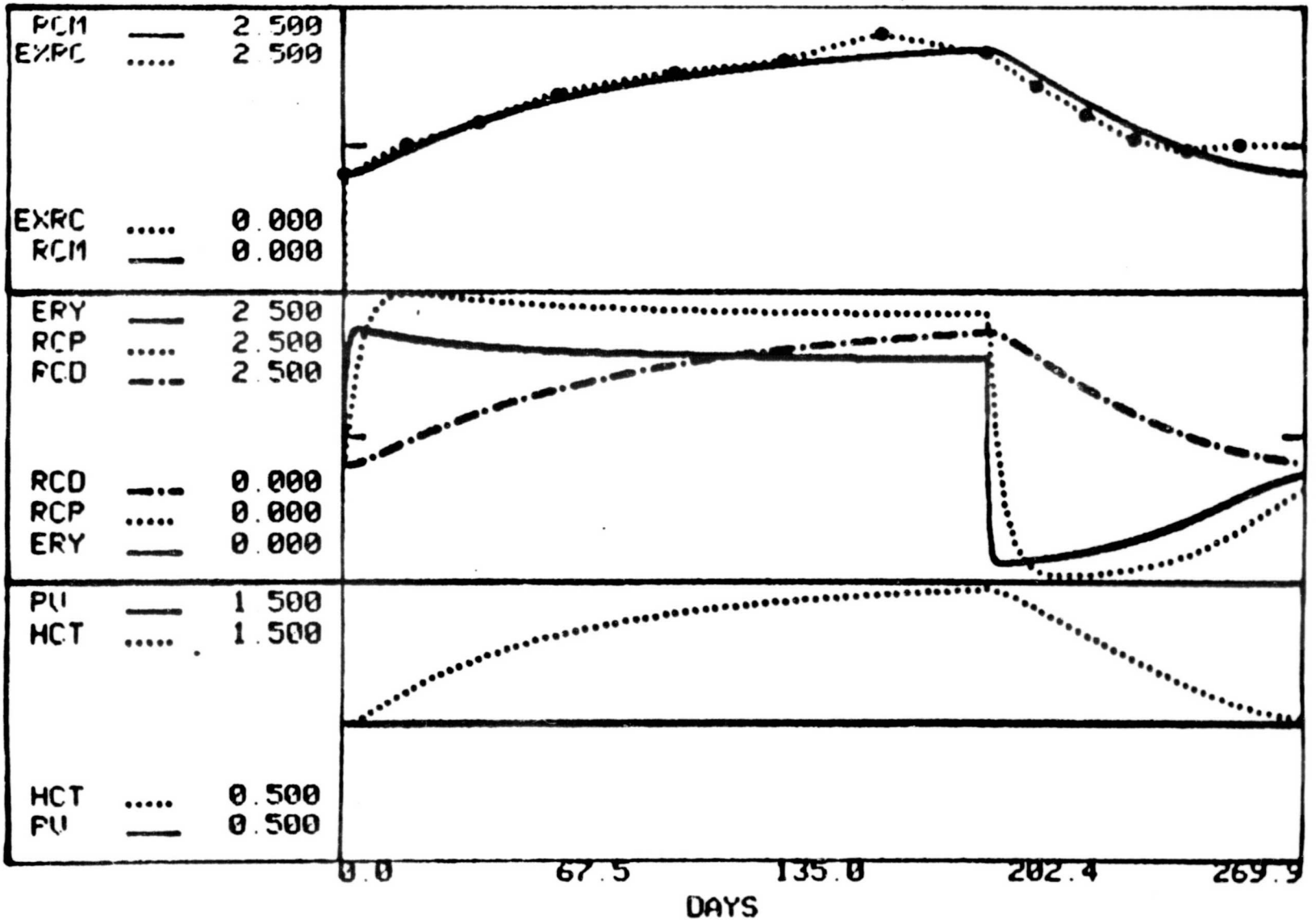

Note: RCM= Red Cell Mass, EXRC= Experimental Red Cell Mass (Buderer & Nace, 6), ERY+ Erythropoietin Concentration, RCP= Red Cell Production, RCD= Red Blood Cell Destruction, PV= Plasma Volume, and HCT= Hematocrit.

an increase in the circulating red blood cell mass (1). The opposite response for the descent phase is also shown. The difference between production and destruction rates in the simulation provide a visual indication of the magnitude of the stress that drives the system from the normal steady-state. The slow approach to equilibrium at altitude that is seen experimentally is evident in the simulation from the asymptotic nature of the model response to the hypoxic stress. Upon return to sea level, the increased hematocrit serves as a prolonged stimulus for tissue hyperoxia to the extent that red cell production is predicted to be totally inhibited for several weeks.

In order to obtain the agreement between normalized red cell mass and the normalized experimental red cell mass shown in Figure 2, two different values for the overall controller gain, G, (i.e., the product of G_1, gain, renal erythropoietin production and G_2, gain of marrow RCP) were required. A value of 2.2 was used during the altitude phase, while a value of 12.0 was required during the descent phase of the simulation. These values for G concur with the results obtained by Leonard et al. (1) for the validation of the original model of erythropoiesis. This difference in effective gains may reflect other circulatory ventilatory and biochemical adjustments that are known to occur in response to disturbances in oxygen transport. While some of these other factors could be simulated using this model, for the purposes of these simulations only the overall gain, G, was changed. The qualitative and quantitative response of the reformulated model to the identified hypoxic stress, along with the use of identical controller values, verifies and revalidates the model.

2.2.1.2 Squirrel Monkey Model Validation. The squirrel monkey version of the model was validated in the same fashion as the human model and against the same data (8). The results of this validation simulation is shown in Figure 3. In the squirrel monkey simulation, P_aO was reduced from the normal value of 85.2 mmHg at sea level to 44.8 mmHg, in order to simulate exposure to an altitude of 3800 m. Since P_aO was not measured experimentally in the pig-tailed monkey, the P_aO value of 44.8 mmHg was determined by scaling the normal squirrel monkey P_aO value (5) by the equivalent percent decrease that is observed to occur in humans for the same altitude. While this is only an approximation of the true squirrel monkey P_aO at this altitude, it is the most

FIGURE 3. Validation of Squirrel Monkey Model of Erythropoiesis using a simulation of Altitude Hypoxia. The Validation Simulation was based upon an experiment by Buderer and Nace (6) on Pig-tailed Macaca Monkeys. The simulation of Hypoxia was performed by reducing PAO form 85.2 to 45.75 MMHG and G from 6.0 to 2.0. The recovery portion of the simulation was performed by returning PAO to normal. All results have been normalized to a pre-stressed level of 1.0

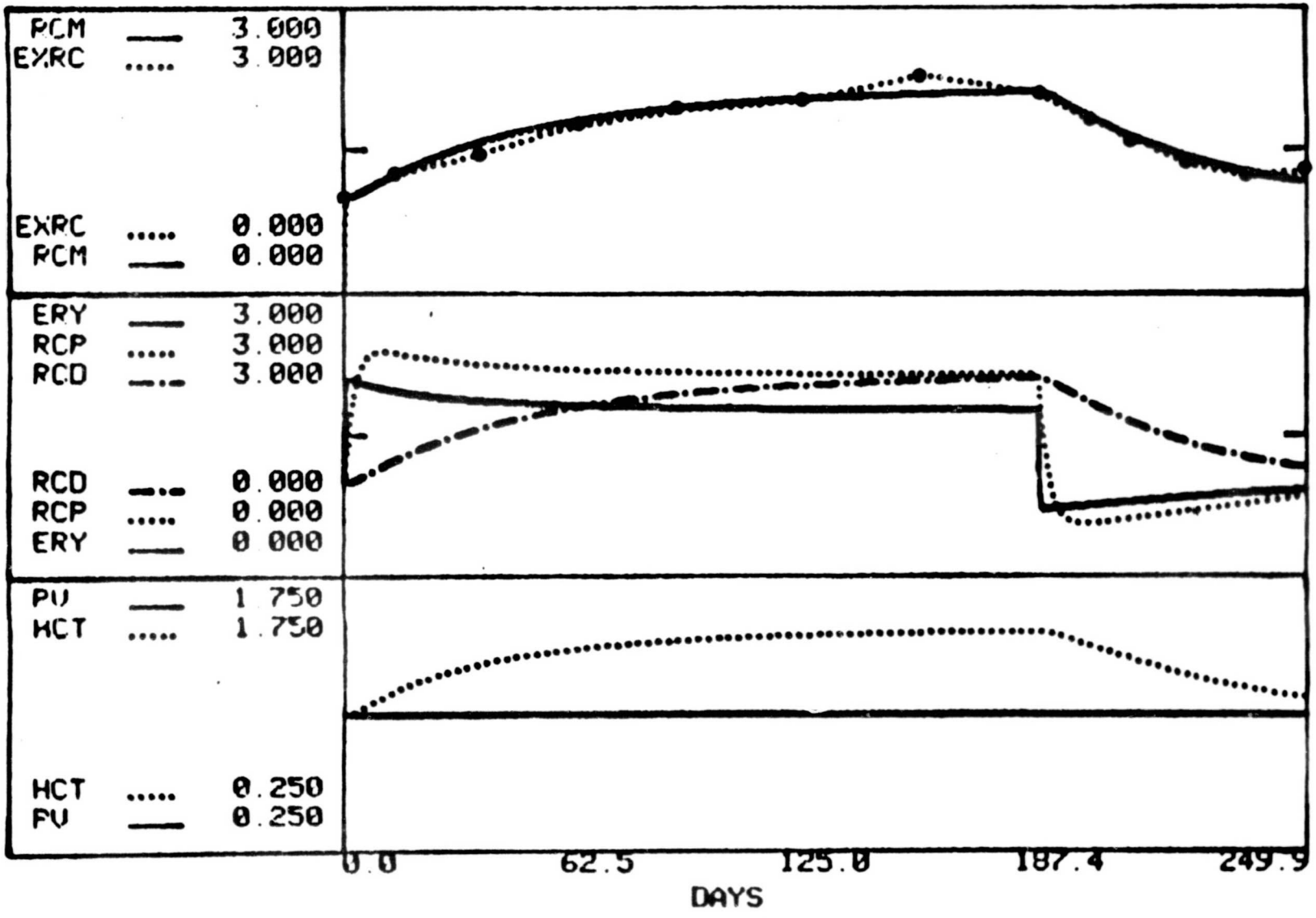

Note: RCM= Red Cell Mass, EXRC= Experimental Red Cell Mass (Buderer & Nace, 6), ERY= Erythropoietin Concentration, RCP= Red Cell Production, RCD= Red Blood Cell Destruction, PV= Plasma Volume, and HCT= Hematocrit.

reasonable estimate available without direct P_aO measurements. As in the human model validation, the overall controller gain, G, was adjusted until the simulation response was in agreement with the experimental red cell mass data. However, unlike the human model, only a single value of G, 2.0, was required to model both the altitude and recovery phases of the simulation. This value of G is in agreement with the G value used during the altitude portion of the human simulation.

2.2.1.3 Rat Model Validation. The rat version of the species-independent model of erythropoiesis was validated against experimental data from Pepelko (12). In this experiment, male Charles River strain rats were exposed to a total barometric pressure of 380 torr (equivalent to an altitude of 5600 m). Rats were sacrificed after 1, 3, 8, 16, and 24 days of exposure to hypoxia and the following hematological measurements taken: red cell mass, hematocrit, and plasma volume. Figure 4 compares the results of the experiment and the model simulation. This simulation was performed by reducing P_aO stepwise from 80.2 to 34 mmHg and by reducing plasma volume from .0056 to .0046 l. Since P_aO was not experimentally determined for these rats, the P_aO of 34 mmHg used in the simulation was obtained by scaling the normal sea-level P_aO value of 80.2 mmHg (5) down by the same percentage change that occurs in a human at the same altitude. Plasma volume was reduced by the same amount observed in the experimental rats during exposure to hypoxia (12). The normalized red cell mass response of the model was adjusted by changing the overall control gain, G, until the simulation results were in agreement with the experimental data. Even though the rat strain used in the simulation model was different from that used in the experimental study, good simulation results were obtained. This could be due to the fact that there is very little hemopoietic difference between the two rat species, and rats used in the simulation and experiment were of approximately the same body weight. For this simulation, a value of 2.0 for the overall controller gain, G, was found to yield the best fit to the experimental red cell mass data.

2.2.1.4 Mouse Model Validation. The mouse version of the species-independent model was validated against experimental data from Mylrea (13). In this experiment, female ICR Swiss Webster strain mice were placed in hypoxic chambers in which they were exposed to an atmosphere of 360 torr to simulate

FIGURE 4. Validation of Rat Model of Erythropoiesis using a simulation of Altitude Hypoxia. The Validation simulation was based upon an experiment by Pepelko (7) on male Charles River Strain Rates. The simulation of Hypoxia was performed by reducing PAO for 80.4 to 34.0 MMHG, PV from .0056 to .0046, ANG G from 6.0 to 2.2. All results have been normalized to a pre-stressed level of 1.0.

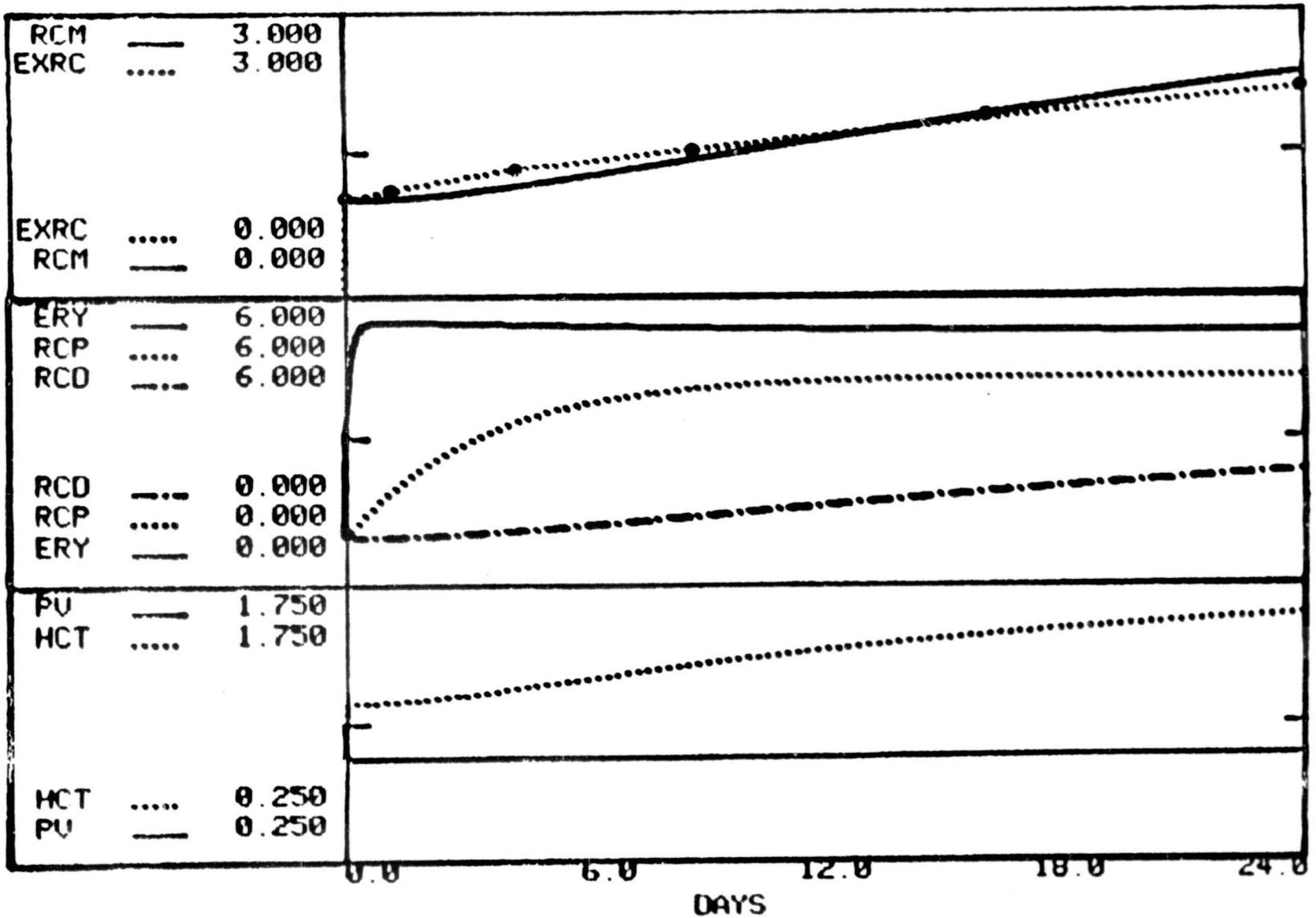

Note: RCM= Red Cell Mass, EXRC= Experimental Red Cell Mass (Pepelko, 7), ERY= Erythropoietin Concentration, RCP= Red Cell Production, RCD= Red Blood Cell Destruction, PV= Plasma Volume, and HCT= Hematocrit.

an altitude of 6000 m. Mice were sacrificed at periodic intervals to show the time course of change in hematocrit, reticulocytes, hemoglobin concentration, blood volume, red cell mass, and plasma volume. The simulation of this experiment was performed by decreasing P_aO from 78 to 29 mmHg and by decreasing plasma volume from .00077 to .00064 l. Since P_aO was not experimentally determined in the mice, the P_aO of 29 mmHg which was used in the simulation, was based on the percent change in human P_aO that is known to occur at the same altitude. The plasma volume decrease was based on the percent decrease that occurred in the experiment (13). The results of this simulation are shown in Figure 5, along with the experimental red cell mass data. The overall controller gain, G, was adjusted until the simulated normalized red cell mass agreed with the experimental data. The best fit occurred at a G level of 1.0.

2.2.2 Discussion on Model Validations

All four validation studies required overall controller gain factors between 1.0 and 2.2 for the hypoxia portion of the simulations. This indicates that the species-independent model of erythropoiesis provides a good overall representation of the physiology for these species. The fact that the human model required a significantly different value of G, overall controller gain, for the recovery phase of the simulation may be due to the fact that the simulation was being compared with primate data. This difference in G values may have to do with the differences in the location of the normal operating point on the oxyhemoglobin dissociation curve between man and the squirrel monkey (see the discussion on steady-state sensitivities, Figure 22). With the normal operating point for the two species falling in different areas of the oxyhemoglobin Equilibrium curve, it is expected that the two species would respond somewhat differently to an hypoxic stress, with the human response less dramatic than the squirrel monkey. If human data were available to compare with the simulation results, a different value for G during the recovery phase may not be necessary. Further experimental work and corresponding validation studies are required in order to clarify the need for different G values or additional modeling work.

FIGURE 5. Validation of Mouse Model of Erythropoiesis using a simulation of Altitude Hypoxia. The Validation simulation was based upon an experiment by Mylrea (8) on female ICR Swiss Webster Strain Mice. The simulation of Hypoxia was performed by reducing PAO from 78.0 to 29.0 MMHG, PV from .00077 to .00064 L, and G from 6.0 to 1.0 All results have been normalized to a pre-stressed level of 1.0.

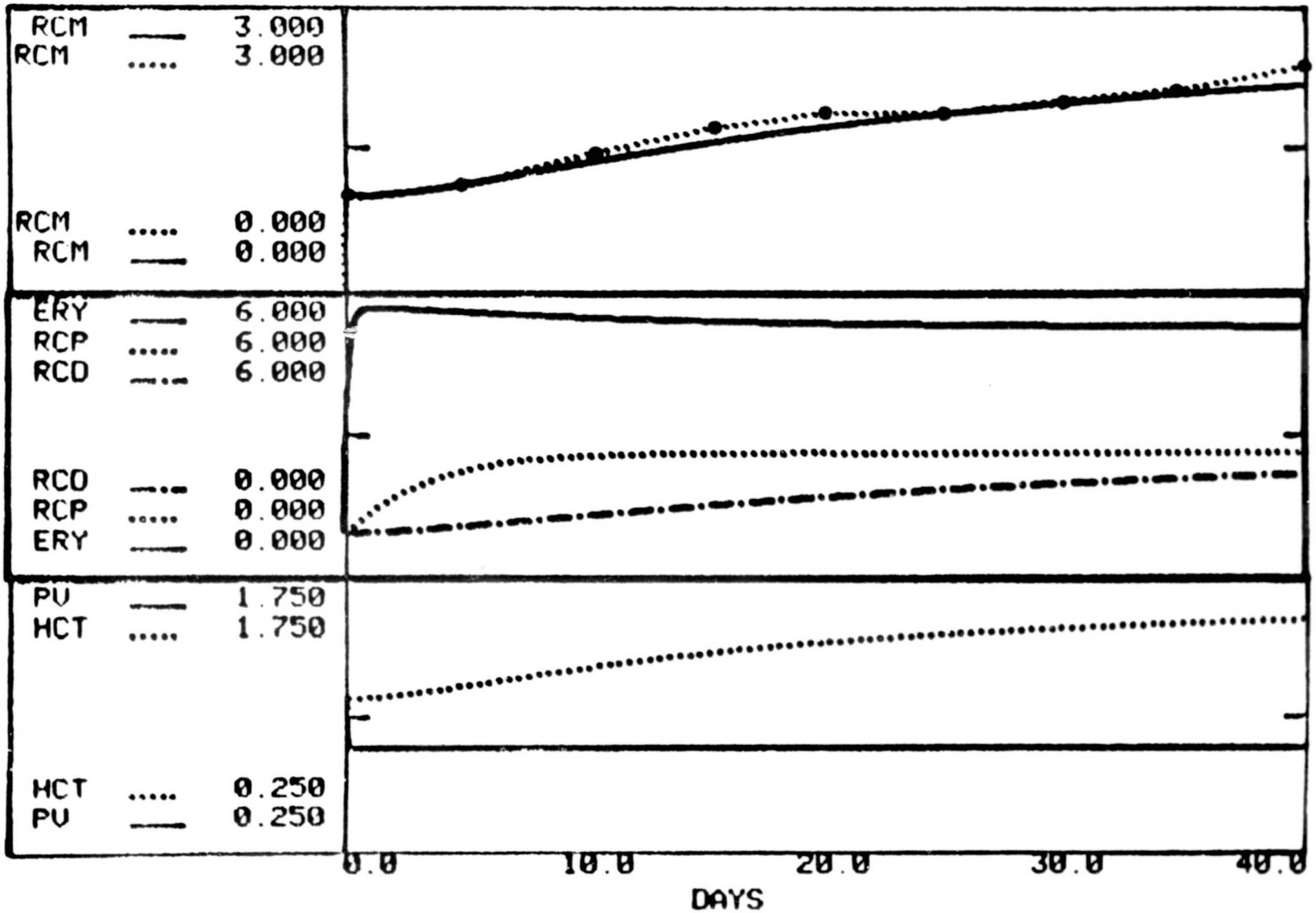

Note: RCM= Red Cell Mass, EXRC= Experimental Red Cell Mass (Mylrea, 8), ERY= Erythropoietin Concentration, RCP= Red Cell Production, RCD= Red Blood Cell Destruction, PV= Plasma Volume, and HCT= Hematocrit.

As discussed previously, other circulatory, ventilatory, and biochemical adjustments are known to occur in response to disturbances in oxygen transport such as exposure to hypoxia, and were not included in these simulations. These regulatory elements can provide partial compensation of tissue hypoxia and may contribute to the finding that in humans erythropoietin returns toward control levels more rapidly than predicted in the simulations shown in Figures 2-5. The erythropoietin response can be more realistically simulated by assuming that changes occur in P_{50}, capillary diffusivity, arterial oxygen tension due to ventilatory compensation, sensitivity of erythropoietin secretion to tissue oxygenation, and sensitivity of erythropoietin responsive cells.

3.0 SPECIES COMPARISON

The primary objective of this study was to compare the erythropoiesis control systems of the human, squirrel monkey, rat, and mouse using the species-specific versions of the erythropoiesis model. This objective was carried out in two parts: first, a detailed sensitivity analysis of how the model functions for each of the four species was performed, and second, the response of the model to a variety of impulse and step stresses relevant to the space-flight program were studied for each species. The following discussion presents of the results of the species comparison study.

3.1 SENSITIVITY ANALYSIS

Using the model formulation discussed earlier, a comparative sensitivity analysis was performed using the species-specific models for the human, mouse, rat, and monkey. Since, in this formulation, species-specific physiology only enters the model through the independent parameters, and since one of the primary issues related to model operation is the effect of parameter changes on the dependent variables, a detailed sensitivity analysis was the logical form for performing both a qualitative and quantitative comparison of the four species models. This analysis was performed on the steady-state and dynamic versions of the model for each of the four species.

3.1.1 Steady-State Sensitivity Analysis

The steady-state sensitivity analysis consisted of parameter-variation studies and the direct analytical determination of steady-state parameter sensivities.

3.1.1.1 Parameter Variation. A parameter-variation study was performed for each species by plotting the new steady-state solutions of the model equations obtained when each of the mathematical and physiological parameters were varied from 50 to 150 percent of their normal values. Figures 6 through 9 present the results obtained for variable X (red cell mass) for each of the major mathematical parameters (A,B,C, and D) with each figure representing results for the human, squirrel monkey, rat, and mouse, respectively. Figures 10 through 13 present similar results, but for variable Y (erythropoietin

FIGURE 6. Effects of variation in the Mathematical Parameters on the Normalized Red Cell Mass (Human)

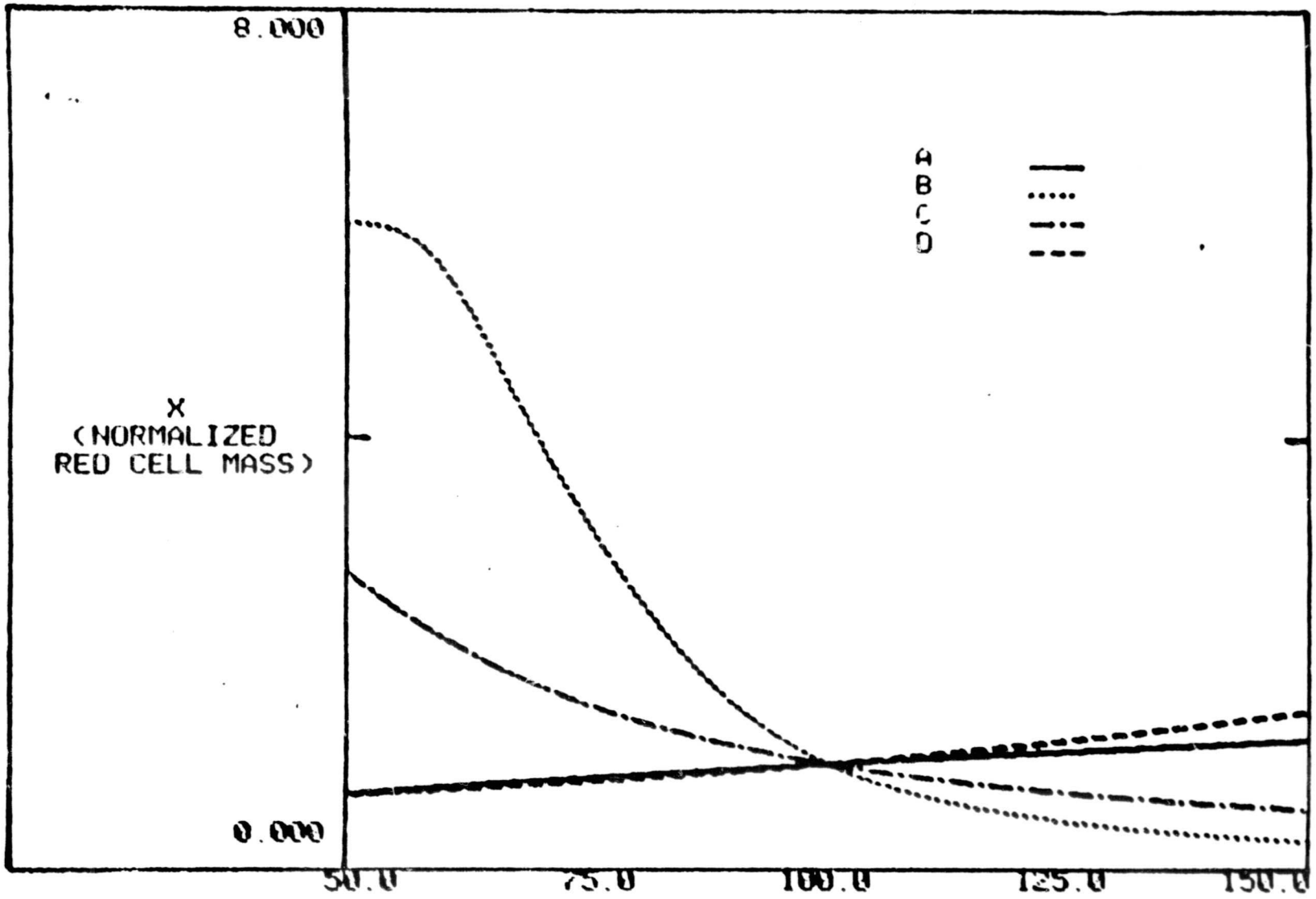

FIGURE 7. Effects of variation in the Mathematical Parameters on the Normalized Red Cell Mass (Squirrel Monkey)

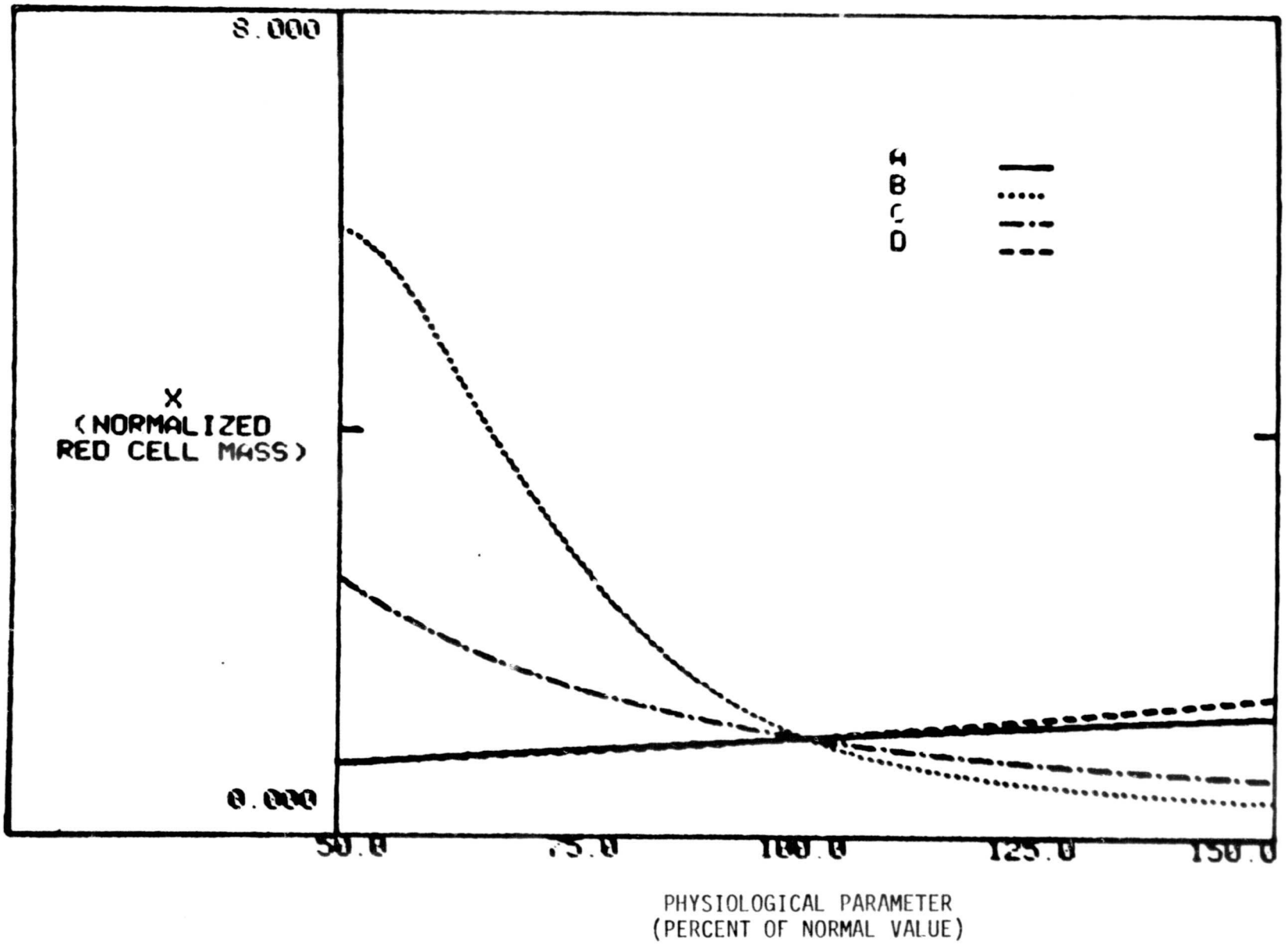

FIGURE 8. Effects of variation in the Mathematical Parameters on the Normalized Red Cell Mass (Rat)

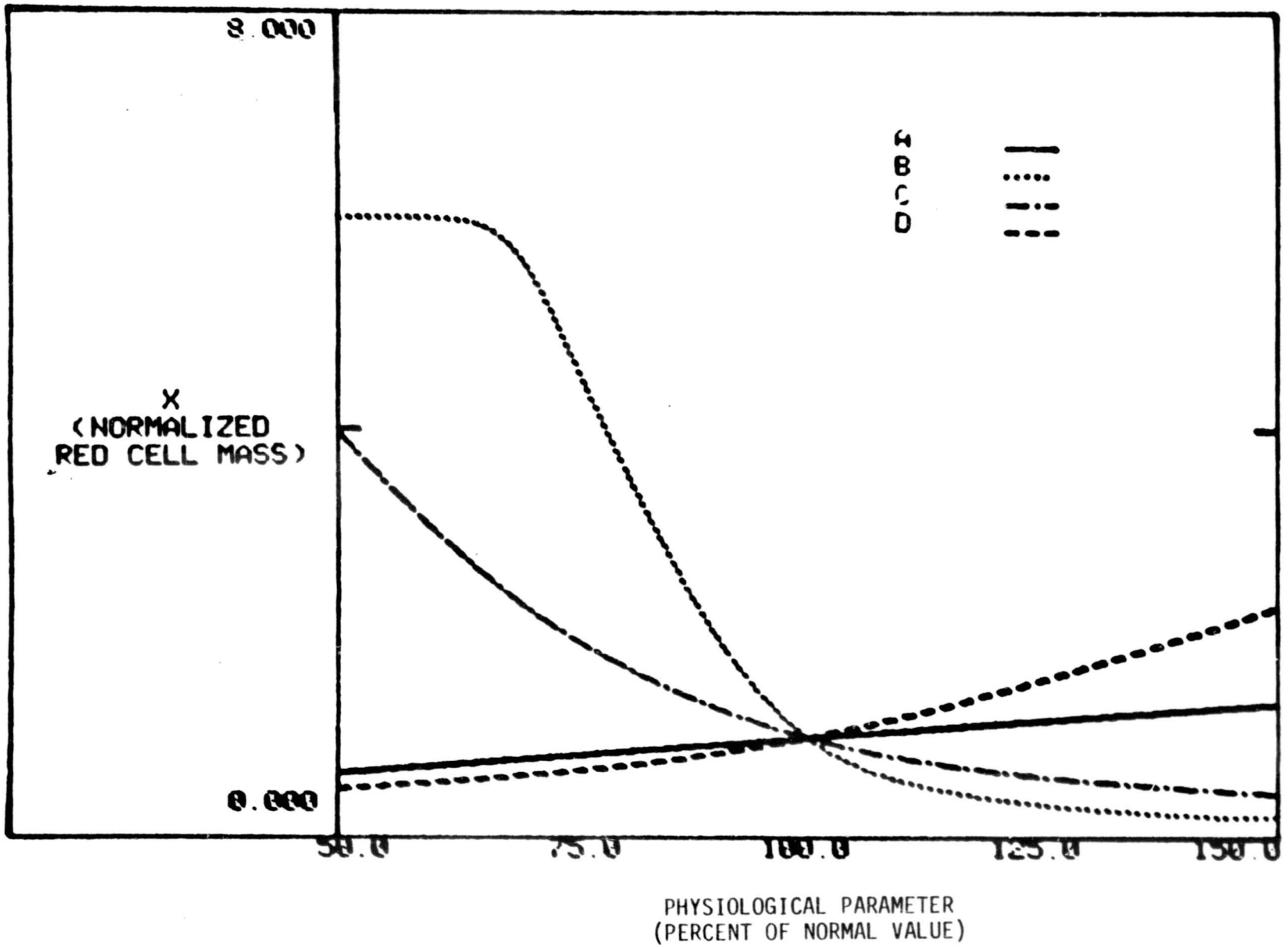

FIGURE 9. Effects of variation in the Mathematical Parameters on the Normalized Red Cell Mass (Mouse)

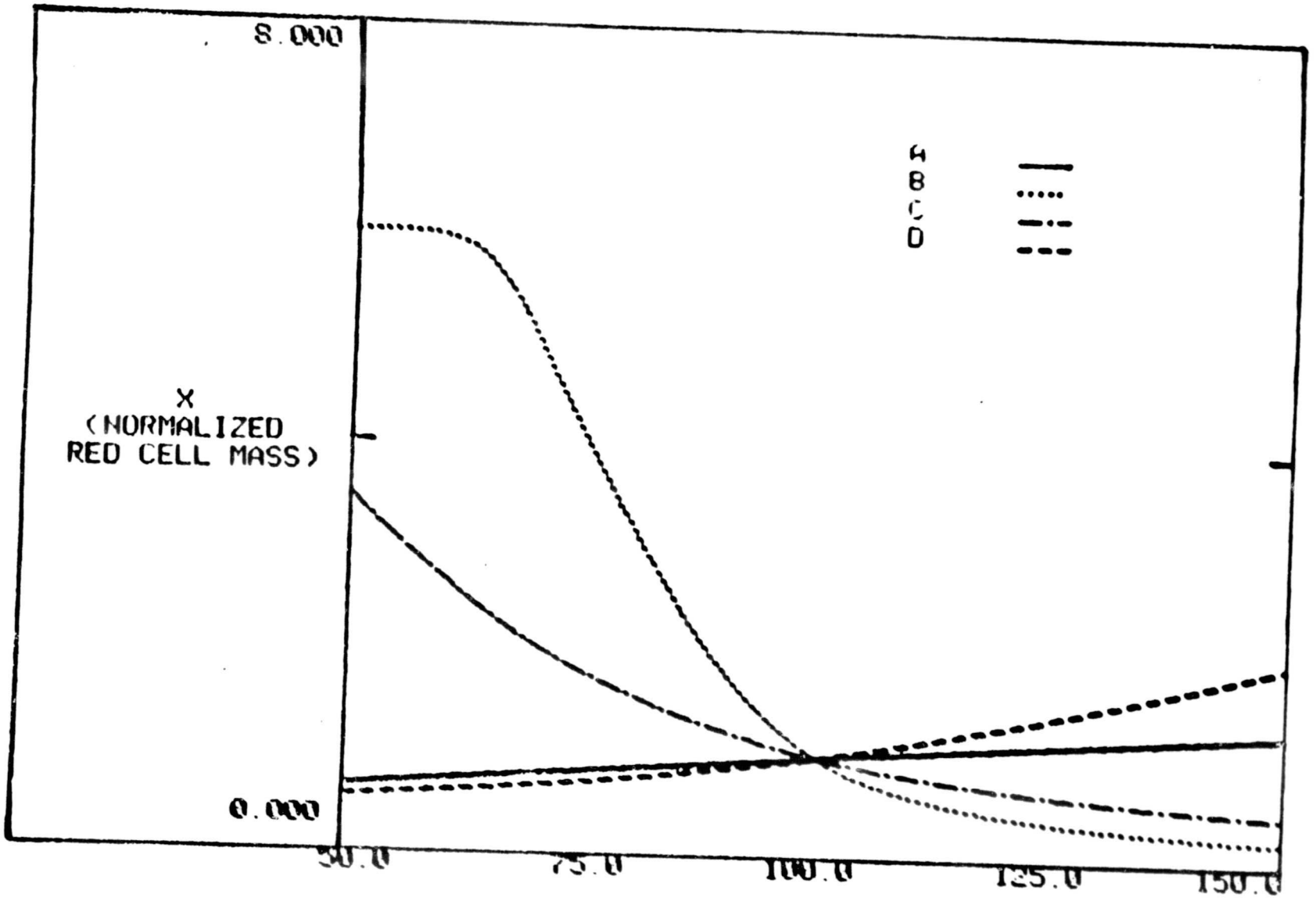

FIGURE 10. Effects of variation in the Mathematical Parameters on the Normalized Erythropoietin (Human)

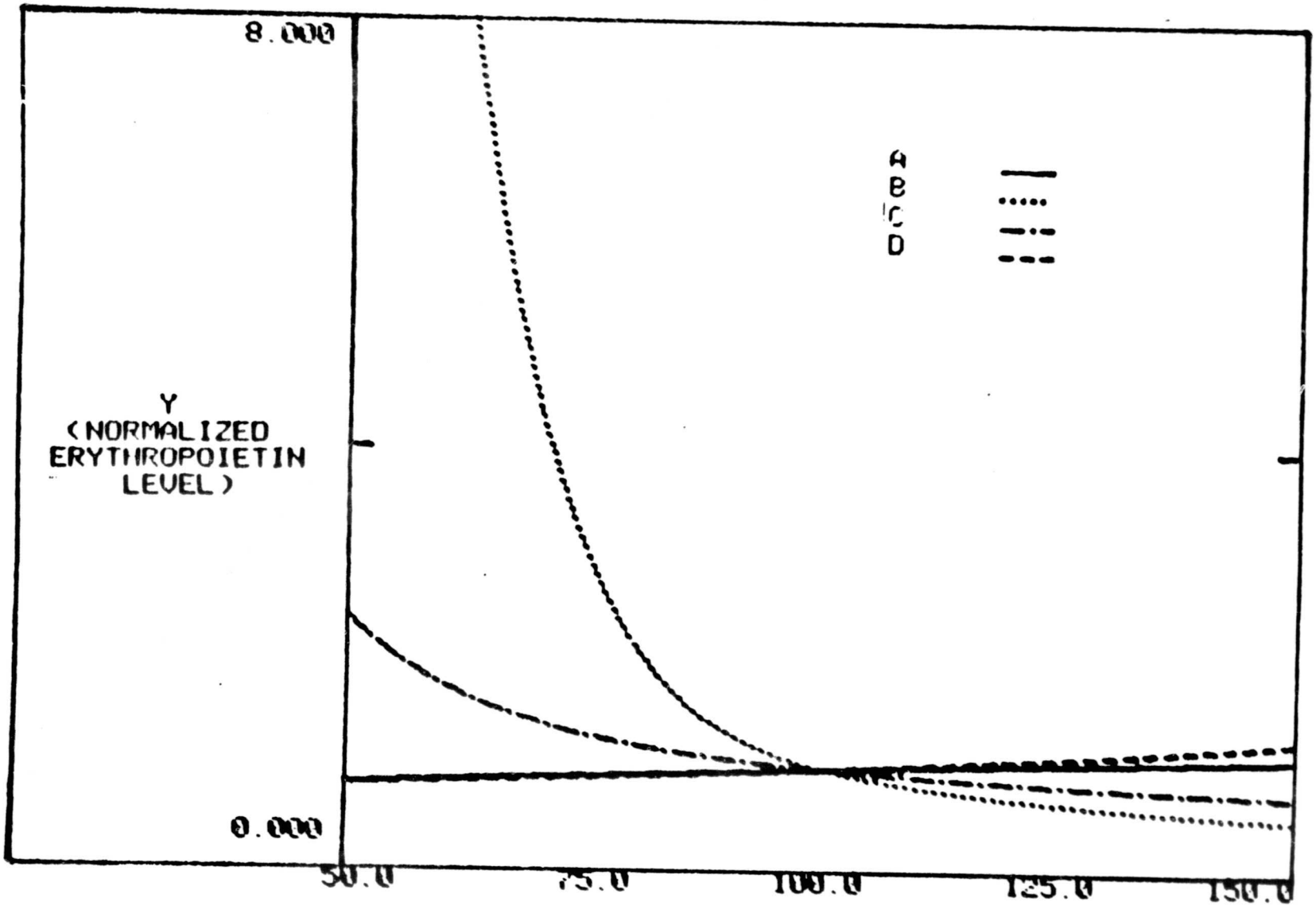

FIGURE 11. Effects of variation in the Mathematical Parameters on the Normalized Erythropoietin (Squirrel Monkey)

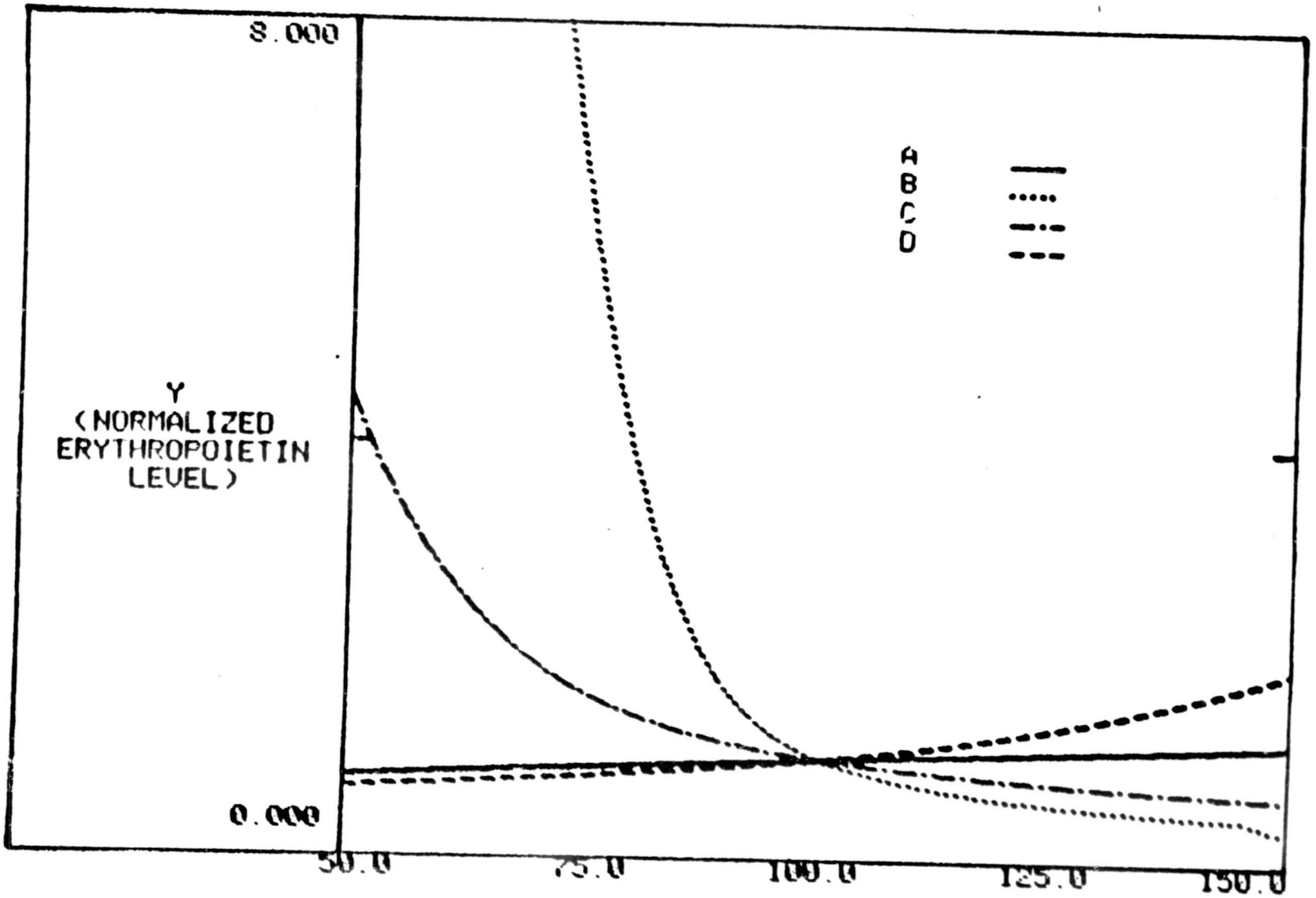

FIGURE 12. Effects of variation in the Mathematical Parameters on the Normalized Erythropoietin (Rat)

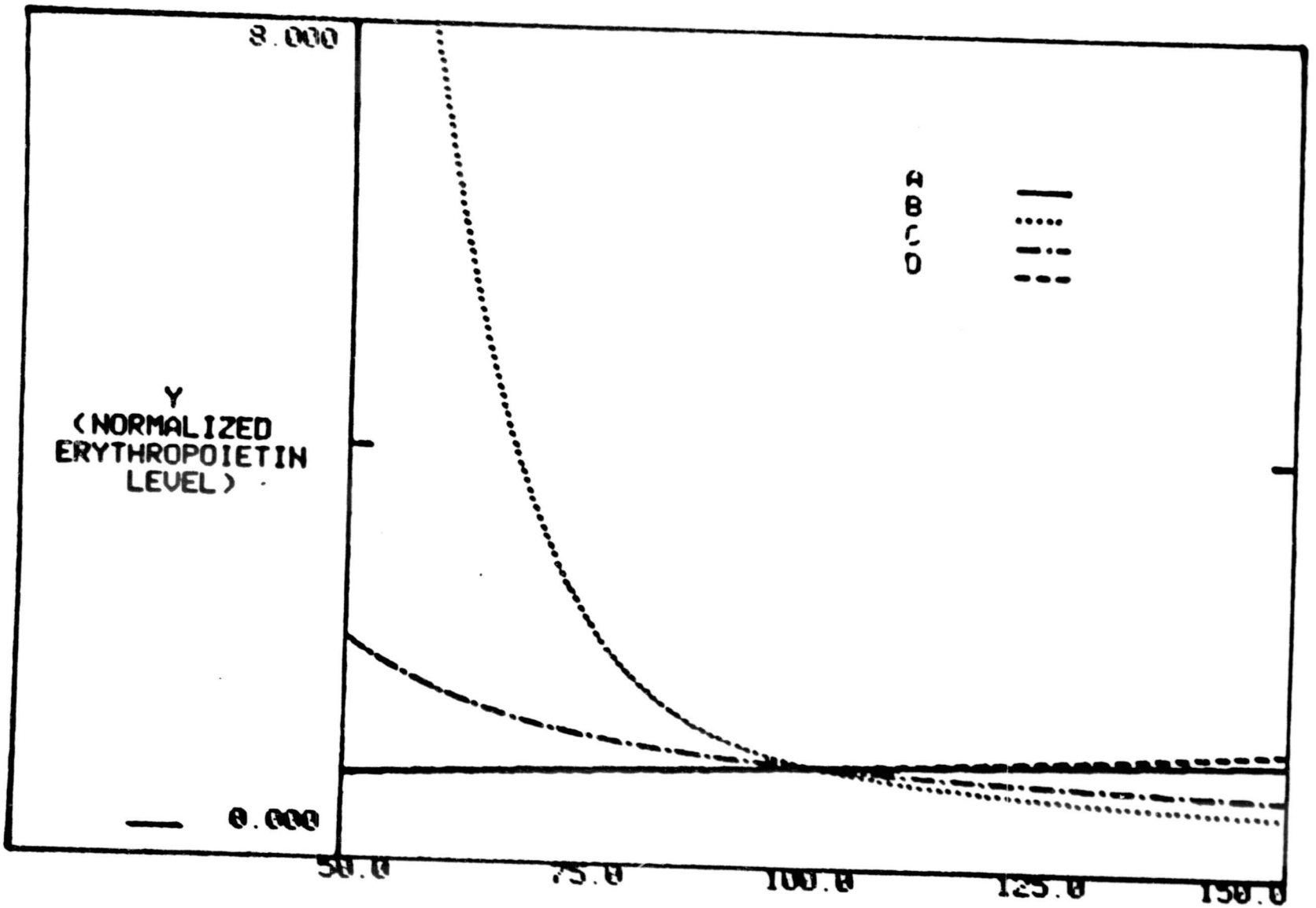

FIGURE 13. Effects of variation in the Mathematical Parameters on the Normalized Erythropoietin (Mouse)

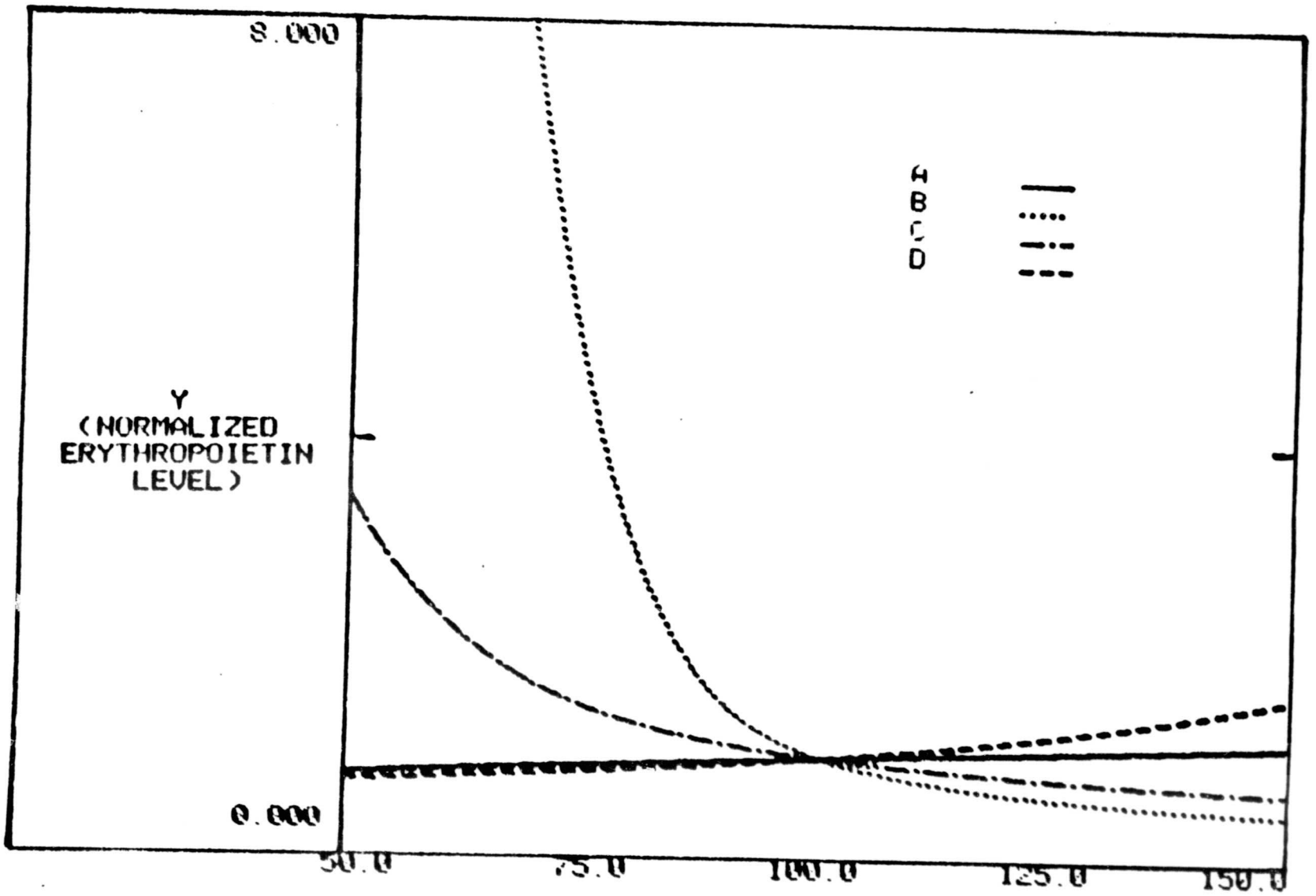

concentration). Since Z = X in the steady state, the effect of parameter variation on Z would be the same as shown in Figures 6-9. In each figure, the curves shown were determined by the actual solution of the model equations.

Figures 14 through 17 and 18 through 21 present the results of the parameter variation study, for the physiological parameters, on the model variables X and Y, respectively. In these cases, the variation of one physiological parameter can affect several of the mathematical parameters, but the numerical approach is no different regardless of the parameters involved. The convergence of the iterative method of solution of the steady-state model equations was always rapid (see section 2.3).

3.1.1.2 Parameter Sensivities. Parameter sensitivities were also calculated for each of the mathematical and physiological parameters. These sensitivities are defined generally as

$$S_p^V = \frac{p_o}{V_o} \left(\frac{\partial V}{\partial p} \right)_o \qquad (25)$$

where V is any dependent variable, p is any parameter, and the subscript o denotes that the right side of equation (25) is evaluated at a normal or reference state. The utility of the above definition arises from the fact that (under suitable mathematical restrictions), for small parameter changes, the parameter sensitivities are the constants of proportionality that directly relate changes in parameter p to changes in Variable V, and that multiple parameter changes are additive, to a first approximation. In other words,

$$\Delta V \simeq \sum_{\ell=1}^{N} S_{p_\ell}^V \cdot \Delta p_\ell \qquad (26)$$

where ΔV represents the fractional change in V and Δp_ℓ represents the fractional change in parameter p_ℓ.

For the multi-species model in the steady state, it is possible to determine the sensitivites analytically. The details of this analytical determination

FIGURE 14. Effects of variation in the Physiological Parameters on the Normalized Red Cell Mass (Human)

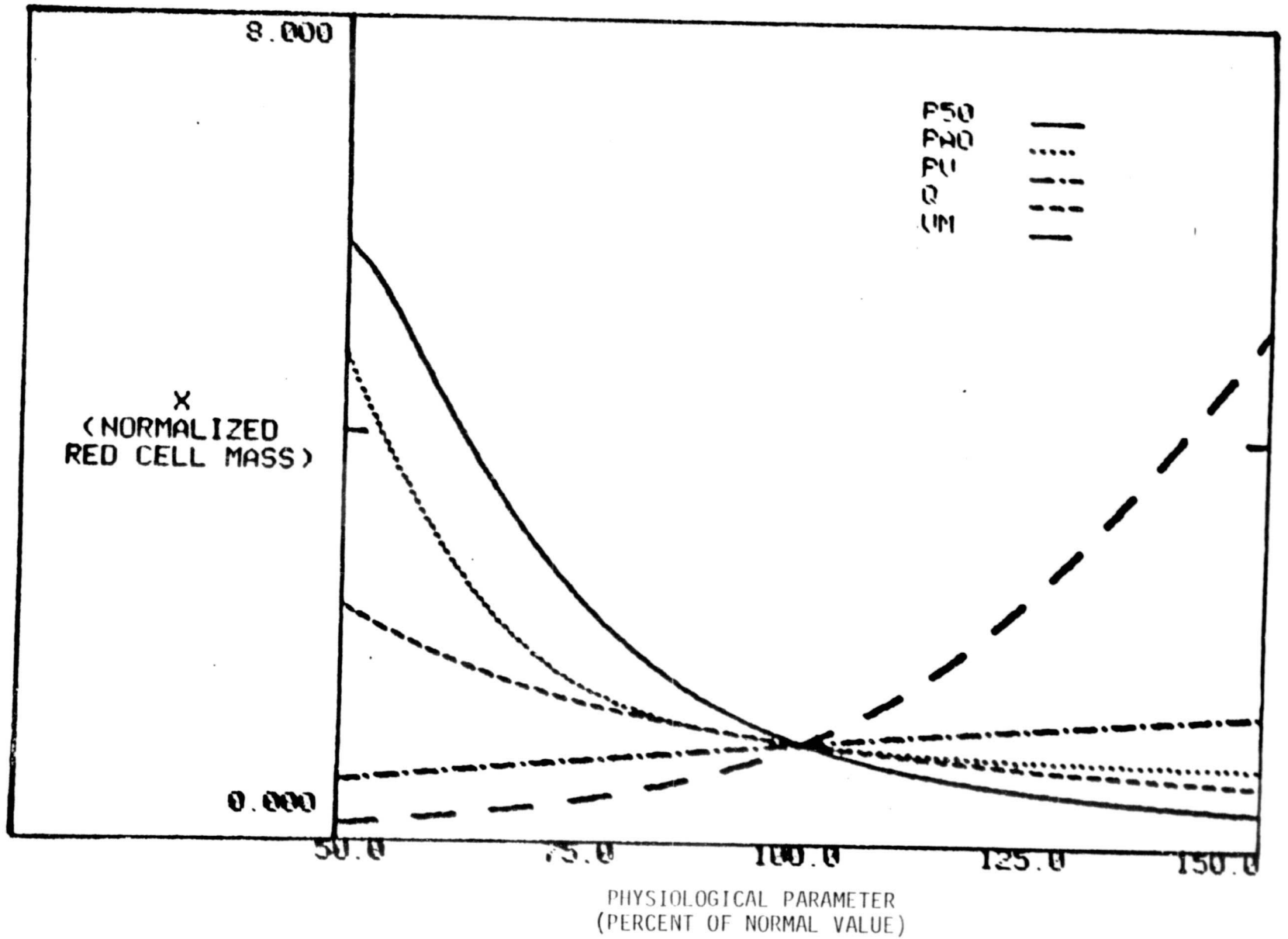

FIGURE 15. Effects of variation in the Physiological Parameters on the Normalized Red Cell Mass (Squirrel Monkey)

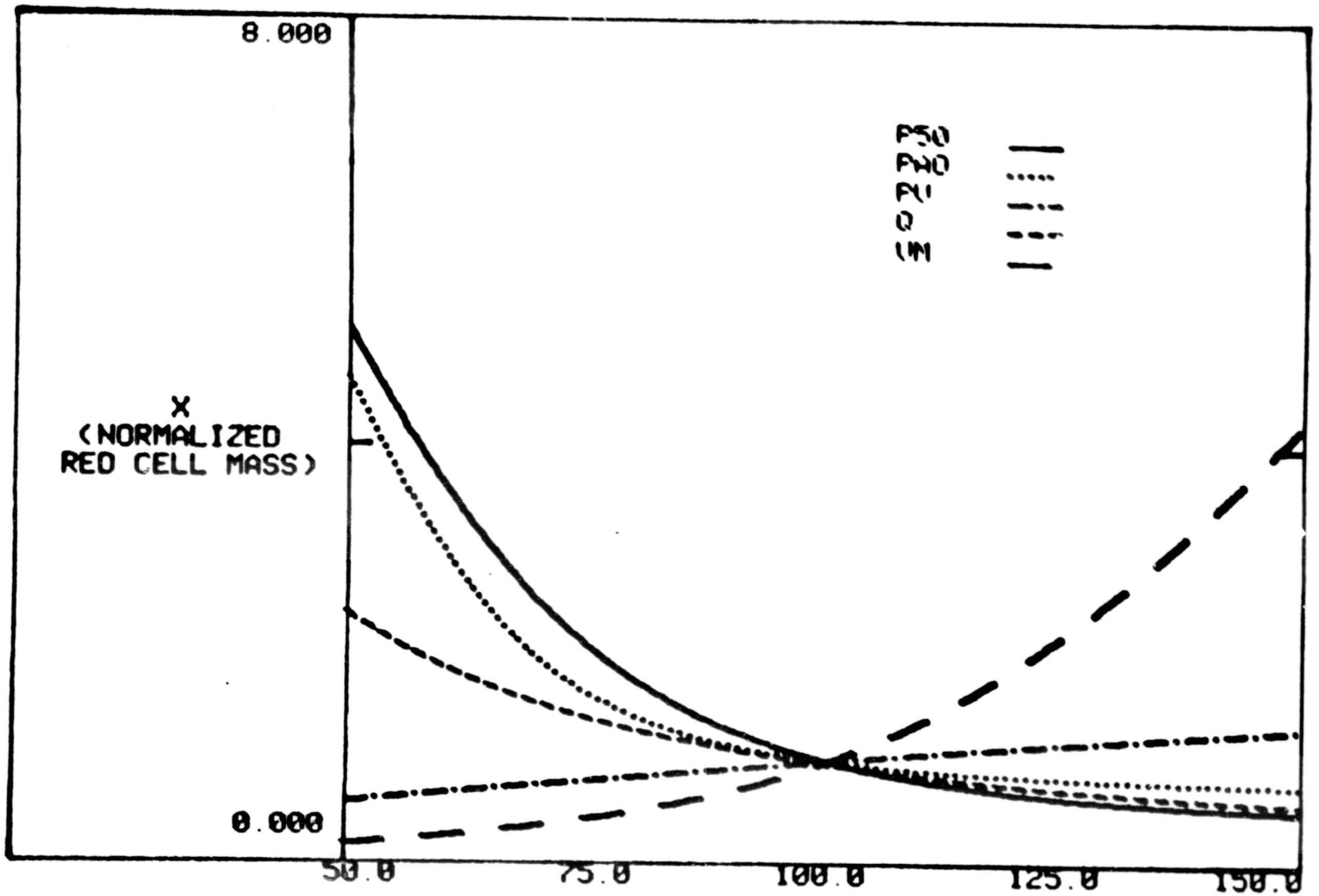

FIGURE 16. Effects of variation in the Physiological Parameters on the Normalized Red Cell Mass (Rat)

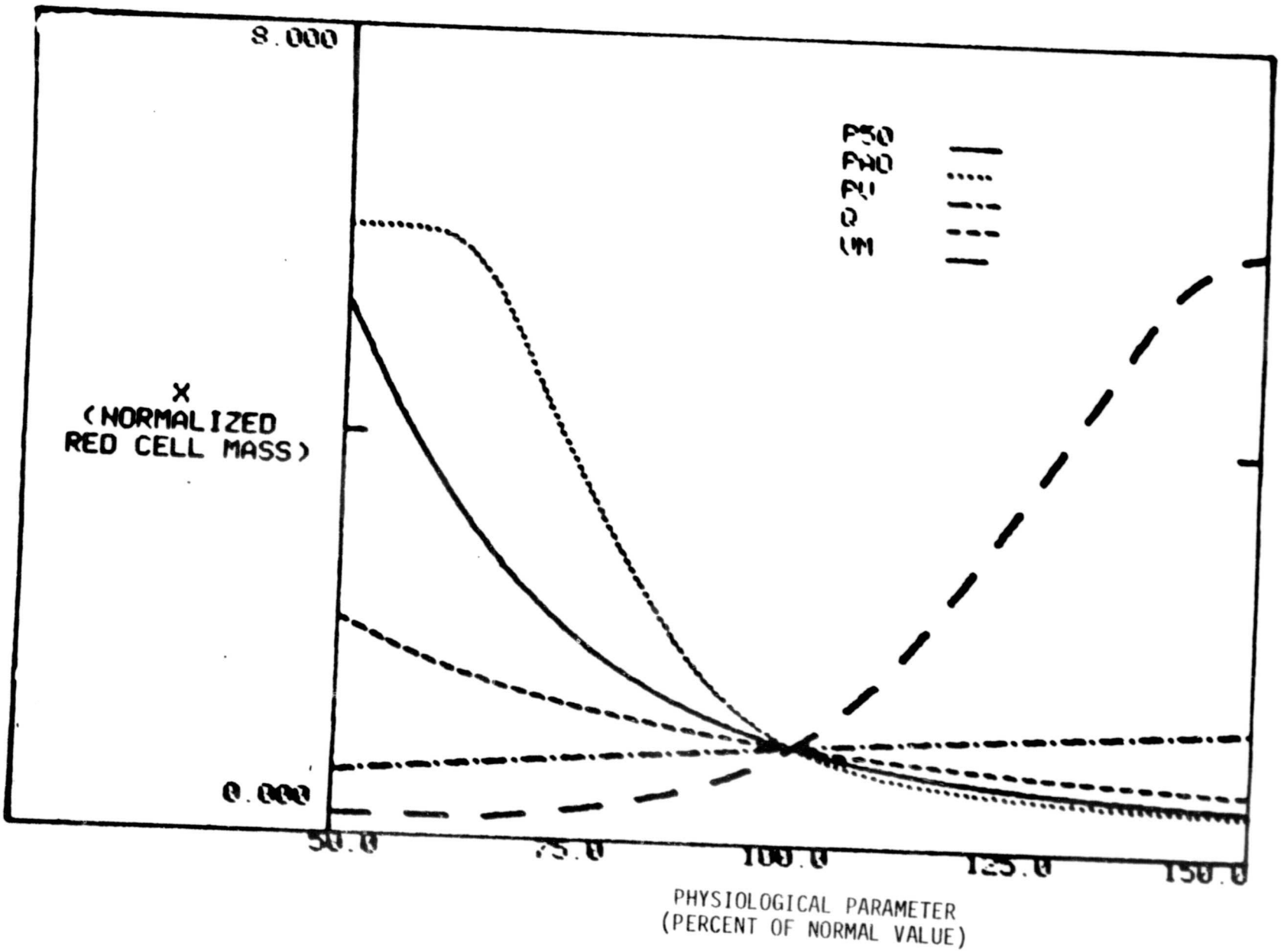

FIGURE 17. Effects of variation in the Physiological Parameters on the Normalized Red Cell Mass (Mouse)

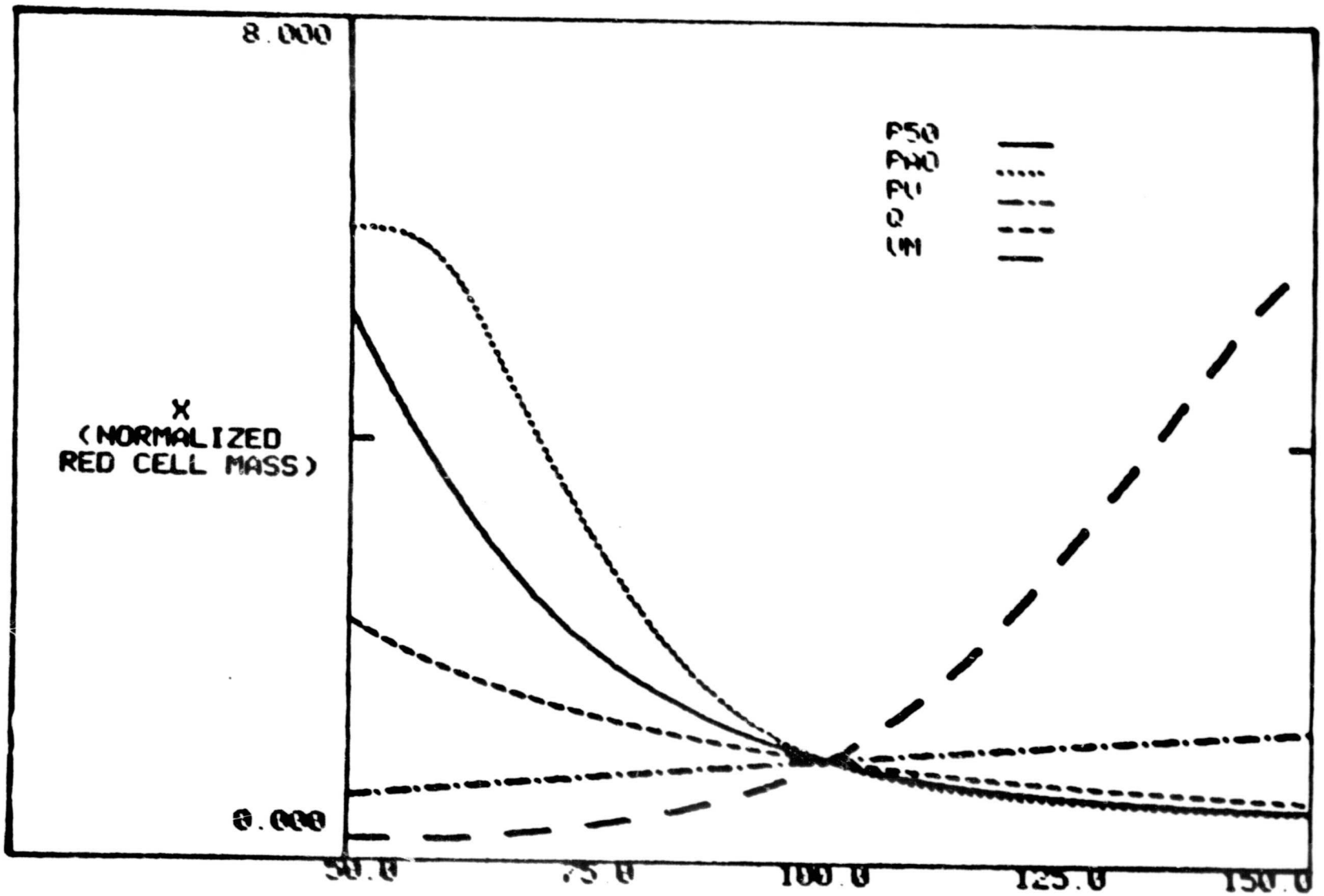

FIGURE 18. Effects of variation in the Physiological Parameters on the Normalized Erythropoietin (Human)

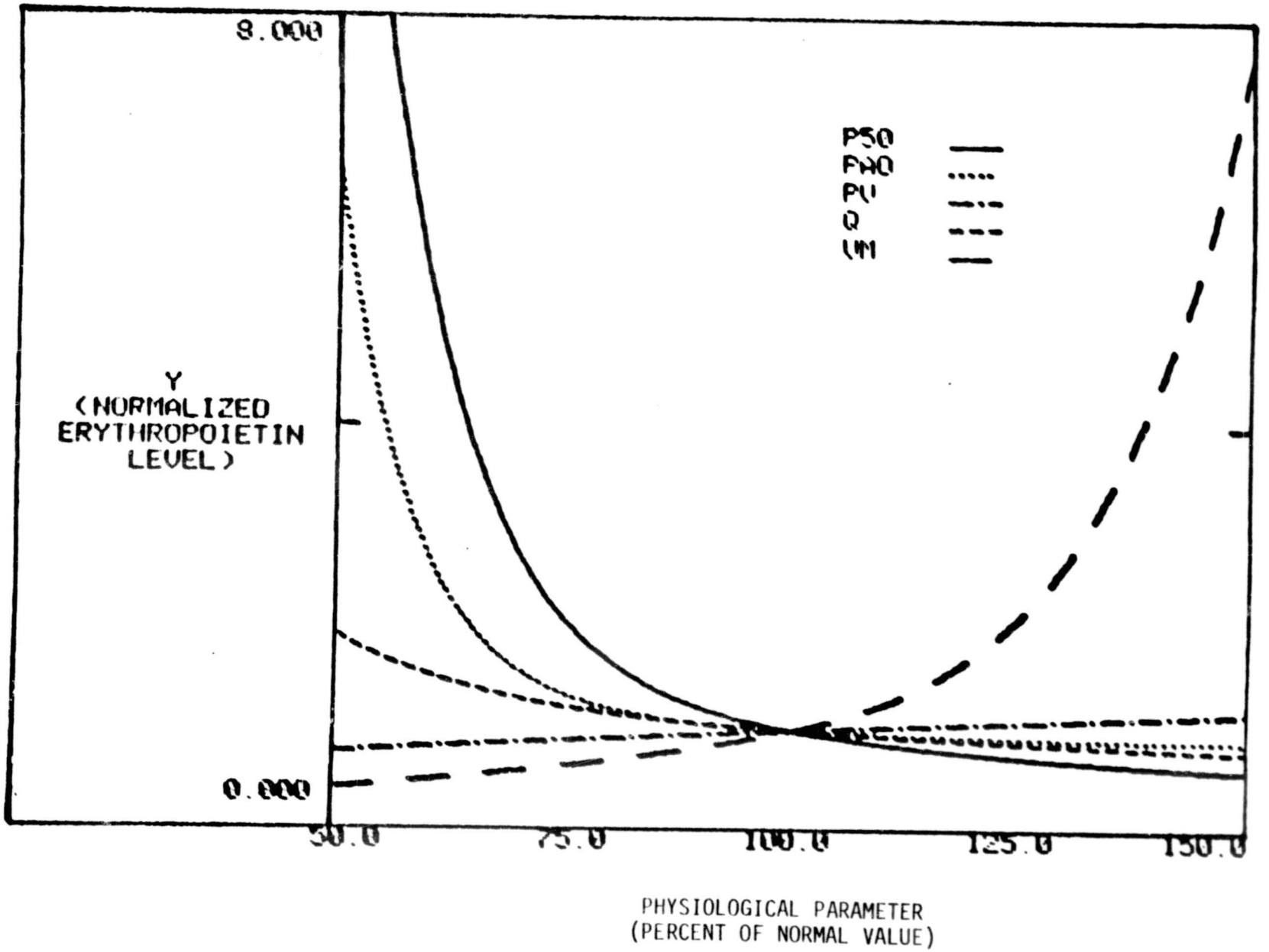

FIGURE 19. Effects of variation in the Physiological Parameters on the Normalized Erythropoietin (Squirrel Monkey)

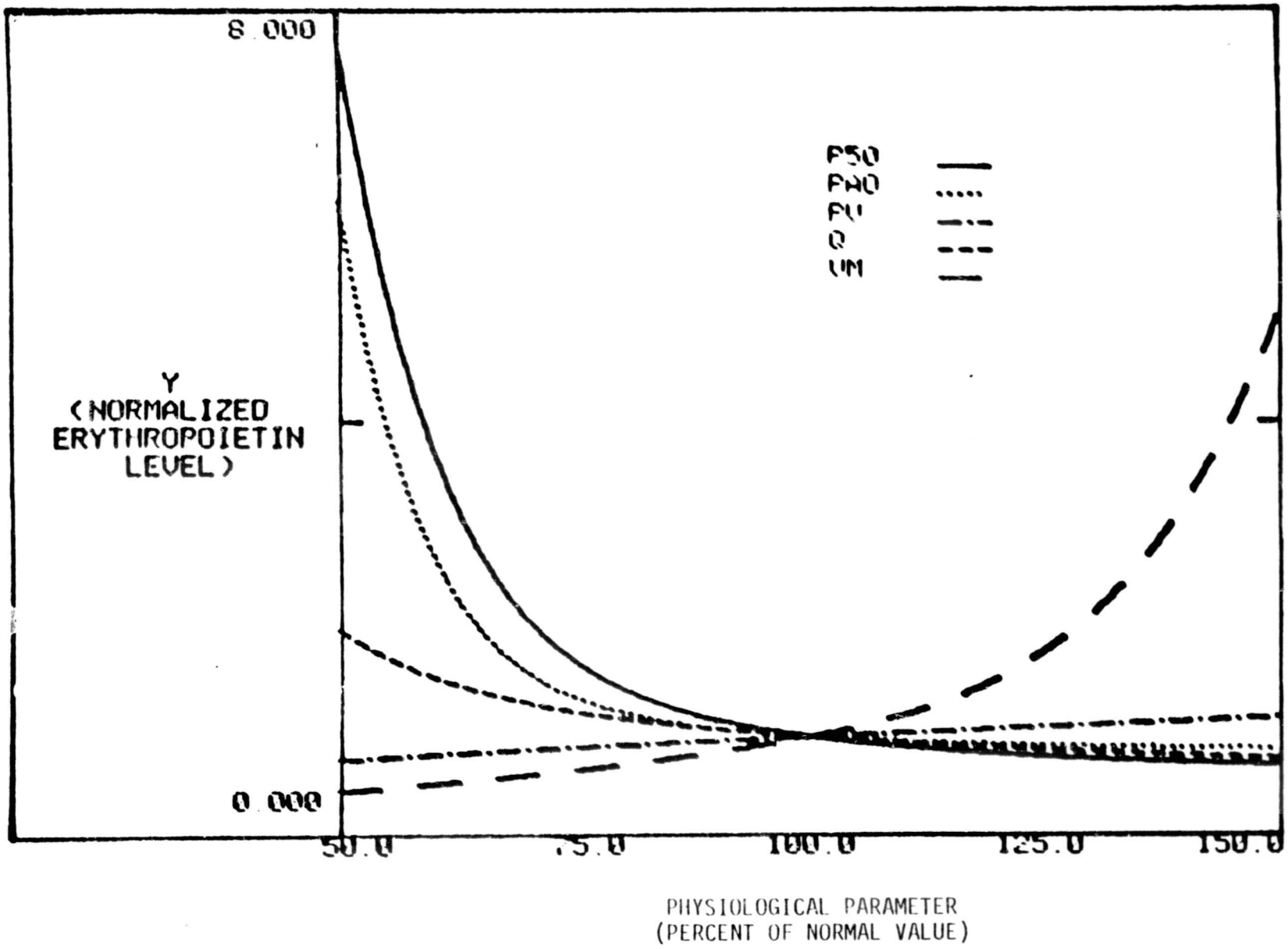

FIGURE 20. Effects of variation in the Physiological Parameters on the Normalized Erythropoietin (Rat)

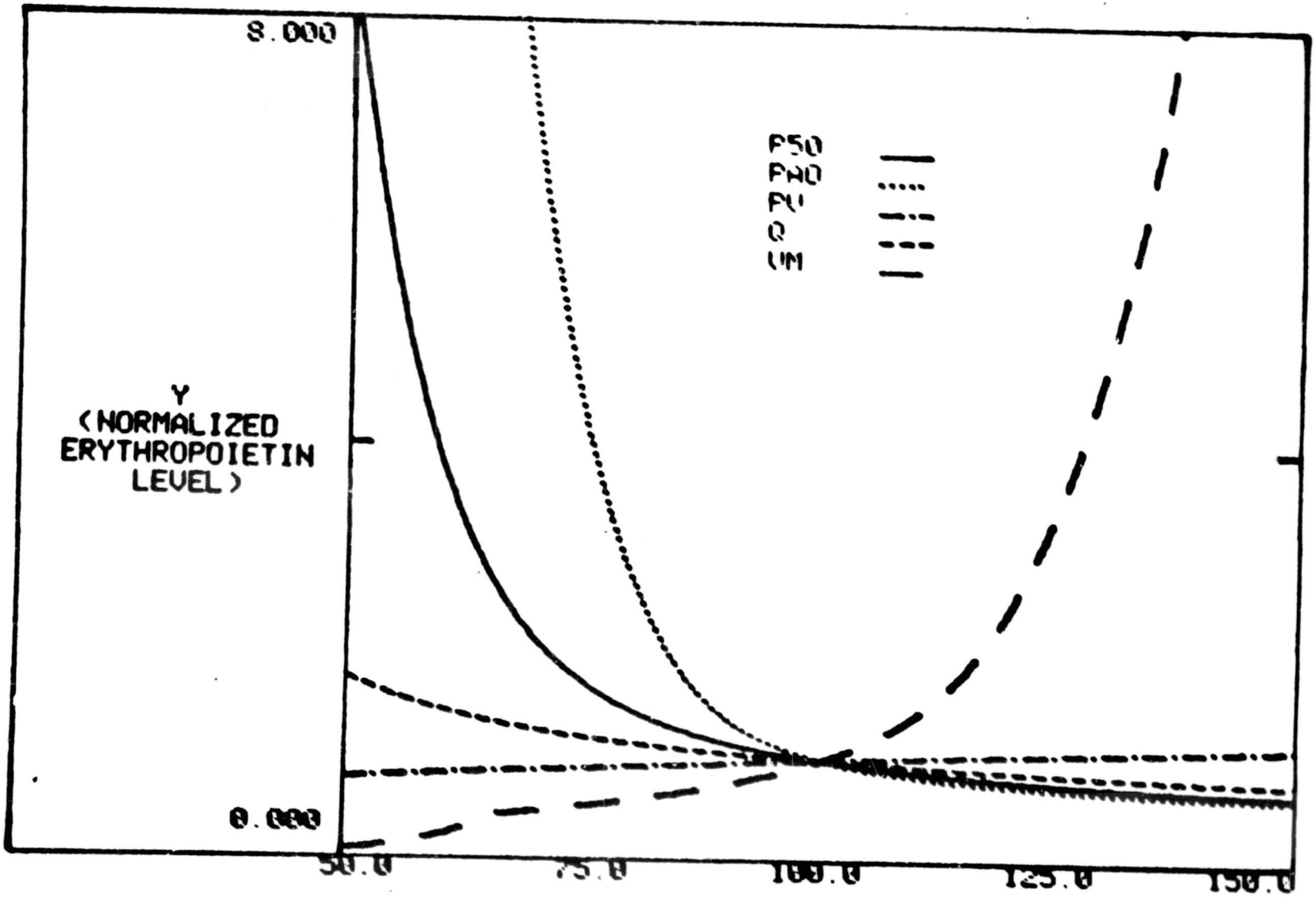

FIGURE 21. Effects of variation in the Physiological Parameters on the Normalized Erythropoietin (Mouse)

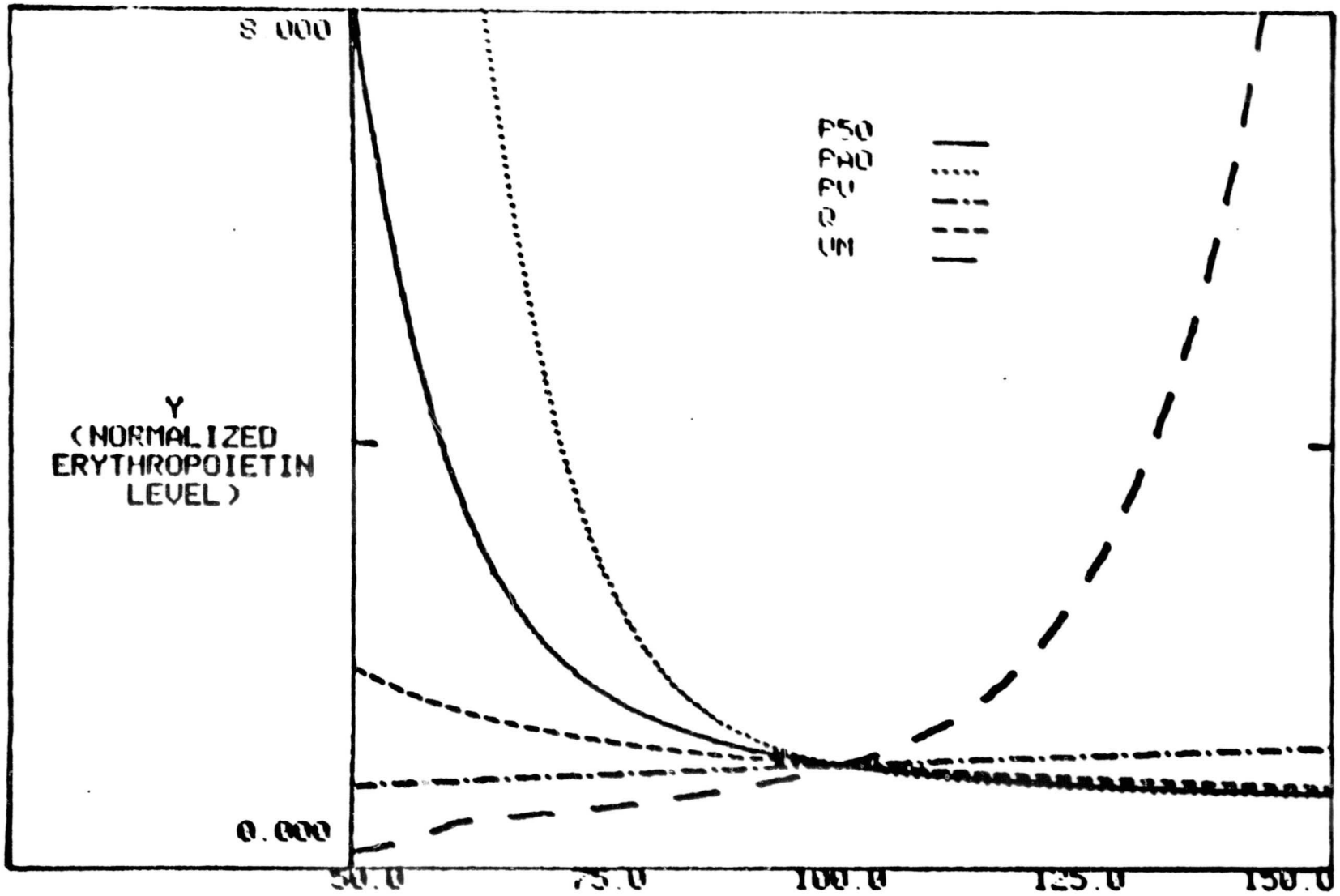

for both the mathematical and the physiological parameters can be found in Appendix A. The sensitivities for each species with respect to mathematical and physiological parameters are given in Tables 4 and 5, respectively. Note that these sensitivities are (essentially) the slopes of the parameter variation curves (Figures 6 through 21) about the normal operating point (Reference State), a fact utilized in less tractable situations to estimate the sensitivities. The values of the slopes were used to verify the values of the sensitivity coefficients determined analytically. The sensitivity coefficients can be used to rank model parameters, both mathematically and physiologically, according to the relative influence that changes in each parameter have in determining the new steady-state solutions. Tables 6 and 7 show the relative ranking of the mathematical and physiological parameters according to how sensitive the model solutions are to changes in parameter values (a ranking of one indicates the parameter to which the model is most sensitive).

3.1.1.3 Discussion on Steady-State Sensitivities. The results from steady-state analysis showed that the model exhibits non-linear parameter dependence for all four species. However, it also showed that over the range of red cell mass that contains physiologically meaningful information (that is, $\pm$50 percent of normalized red cell mass), the model responds in an approximately linear fashion. This is important because the parameter sensitivities can be used to estimate new values of red cell mass and erythropoietin concentration, not only for small changes in a single or combinations of parameters (that is, changes of less than 5%), but also to accurately estimate steady-state solutions for moderate changes (5 to 10%) in the parameter values without the need of an iterative solution scheme as shown in Equation 26.

The steady-state sensitivity analysis allows the model parameters to be ranked according to the impact that changes in parameter value have on the steady-state solutions, and to identify how those solutions vary between species. If the erythropoietic systems show identical responses to parameter changes (that is, if the mouse, rat, and squirrel monkey are perfect models of human erythropoiesis), the mathematical parameters should be identical, even though the specific physiological parameters would be expected to be

Table 4. Steady-State Sensitivity Coefficients for Major Mathematical Parameters

SYMBOL	HUMAN		SQUIRREL MONKEY		RAT		MOUSE	
(P)	SPX	SPY	SPX	SPY	SPX	SPY	SPX	SPY
A	0.5779	.1445	0.4877	0.2439	0.6997	0.3498	0.6357	0.3179
B	-4.795	-1.1989	-3.524	-1.762	-6.843	-3.421	-5.609	-2.804
C	-1.736	-0.4340	-1.430	-0.7149	-2.455	-1.227	-2.082	-1.041
D	0.8805	0.2201	0.6737	0.3369	1.805	0.9023	1.399	0.6997

Table 5. Steady-State Sensitivity Coefficients For Some Physiological Parameters

SYMBOL	HUMAN		MONKEY		RAT		MOUSE	
(P)	SPX	SPY	SPX	SPY	SPX	SPY	SPX	SPY
KD	-3.061	-0.7654	-2.060	-1.030	-4.744	-2.372	-3.701	-1.851
P50	-3.612	-0.9030	-2.375	-1.187	-2.492	-1.246	-2.355	-1.178
PAO	-1.183	-0.2958	-1.148	-0.5741	-4.350	-2.175	-3.254	-1.627
PV	0.8555	0.2139	0.7561	0.3781	0.6502	0.3251	0.6821	0.3411
Q	-1.426	-0.3565	-1.284	-0.6421	-1.161	-0.5805	-1.2403	-0.6201
VM	4.487	1.128	4.942	2.471	5.905	2.952	4.942	2.471

Table 6. Numerical Ranking of the Steady-State Sensitivity Coefficients For Some of the Major Mathematical Parameters

SYMBOL	HUMAN		SQUIRREL MONKEY		RAT		MOUSE	
(P)	SPX	SPY	SPX	SPY	SPX	SPY	SPX	SPY
A	4	4	4	4	4	4	4	4
B	1	1	1	1	1	1	1	1
C	2	2	2	2	2	2	2	2
D	3	3	3	3	3	3	3	3

Table 7. Numerical Ranking of Steady-State Sensitivity Coefficients For Some Physiological Parameters

SYMBOL	HUMAN		MONKEY		RAT		MOUSE	
(P)	SPX	SPY	SPX	SPY	SPX	SPY	SPX	SPY
KD	3	3	3	3	2	2	2	2
P50	2	2	2	2	4	4	4	4
PAO	5	5	5	5	3	3	3	3
PV	6	6	6	6	6	6	6	6
Q	4	4	4	4	5	5	5	5
VM	1	1	1	1	1	1	1	1

different. In fact, the mathematical parameters calculated for the four models are different, but within the same order of magnitude (see Table 3). The qualitative responses of the four models to independent variations in the mathematical parameter, while slightly different at the extremes of the parameter variation, are similar about the normal operating point (see Figures 6 through 21). The parameter sensitivities for the four models are slightly different; the magnitude and overall ranking of the sensitivities of the mathematical parameters remain the same between the species (see Table 4 and 6). The sensitivity coefficients for the physiological parameters can be grouped into two groups of two species each, based on the magnitude and numerical ranking of the sensitivities. The human and squirrel monkey belong to one of the groups while the rat and mouse belong to the other (see Tables 5 and 7).

The interesting analysis from a physiological point of view is the species-to-species model response to changes in the physiological parameters. Changes in renal blood flow (Q), plasma volume (PV), and renal oxygen uptake (V_m) produce qualitatively the same results in all species. This is confirmed by the magnitude of the sensitivity coefficients for these parameters. However, the model response to changes in arterial oxygen tension (P_aO) and the partial pressure at which hemoglobin is 50 percent saturated with oxygen (P_{50}) varies significantly between species. In fact, the curves actually change positions as body mass decreases (that is, from man down to the mouse, see Tables 5 and 7). This reverse in parameter sensitivities can be traced back to the species difference in the ration of P_{50} to P_aO. The ratio increases as body mass decreases as can be seen in Table 8. This ratio determines the shape of the oxygen-hemoglobin dissociation curve and the location of the operating point on that curve. A change in P_{50} will change the curve shape, a change in P_aO will change the location of the operating point, and a change in either will change the value of arterial oxygen saturation (S_aO) which is used to calculate several of the mathematical parameters. Figure 22 shows the oxygen-hemoglobin equilibrium curve for all four species. Note that arterial oxygen tension decreases and P_{50} increases as body mass decreases. Each of these changes alone cause a small decrease in arterial oxygen saturation; however, the combined changes result in a significant difference in saturation between species with the trend being towards a decrease in saturation as body mass decreases.

Table 8. Ratio of P_{50} to Arterial Oxygen Tension (PAO)
For All Four Species

Species	P50/PAO
Human	.28
Squirrel Monkey	.41
Rat	.47
Mouse	.50

FIGURE 22. Theoretical Oxyhemoglobin Equilibrium Curves for Man, Squirrel Monkey, Rat and Mouse. Curves were generated using the Hill Equation and the Values of P_{50} and k shown in Table 2 for each Species.

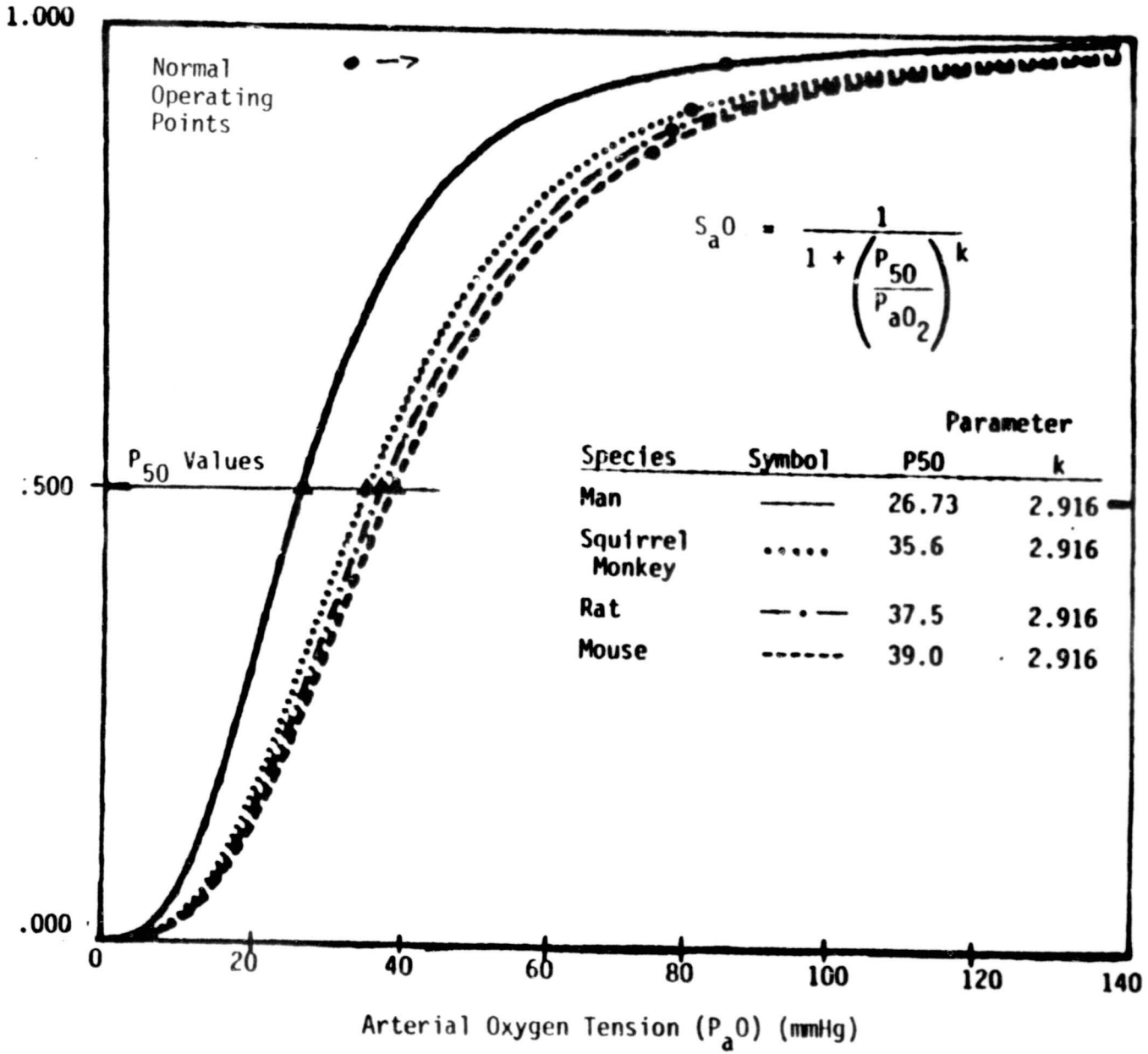

The steady-state sensitivity analysis yielded the following two main results: 1) all four models qualitatively respond the same way to changes in the mathematical parameters, and 2) the models respond qualitatively the same way to changes in all of the major physiological parameters, except for P_aO and P_{50} due to a species difference associated with oxy-hemoglobin dissociation.

3.1.2 Dynamic Sensitivity Analysis

Dynamic sensitivities were calculated for all parameters, both "mathematical" and physiological. Dynamic sensitivities describe how the independent variable values change with respect to changes in parameter values as a function of simulation time. Appendix B provides a brief description and derivation of the equations used to calculate the dynamic sensitivities. Figure 23 shows an example of how the sensitivities for red cell mass (x), erythropoietin concentration (y), and red blood cell production (z), each with respect to the mathematical parameter A, change as a function of simulation time for the human, squirrel monkey, rat, and mouse. The sensitivity curves for x and y show that the model is more sensitive to changes in parameter A early in a simulation where the sensitivities peak in value (0 to 25 days), than later in a simulation where the sensitivities slowly decrease until they are equal to the steady-state sensitivity value. The sensitivity curves for y with respect to A peak sooner than the curves for z. The curves for x, however, show that the sensitivity increases slowly until it approaches the steady-state sensitivity value. Similar results were found for all parameters, both mathematical and physiological, for all four species (see Figures 22 through 28). Figures 23 through 26 show the dynamic sensitivities of x, y, and z for all four species with respect to the mathematical parameters A, B, C, and D. Figures 27 through 29 show how the dynamic sensitivities for variables x, y, and z with respect to the physiological parameters P_{50}, P_aO, PV, Q, and V_m vary between each species. The only major difference between the dynamic sensitivities is that some of the parameters are associated with negative sensitivities. However, the trends for the absolute values of the sensitivities remain the same for all parameters. That is, y and z are more sensitive to parameter changes early in a simulation, while x is more sensitive to parameter changes at the end of a simulation. These trends are related to the time constants K1, K2, and K3 association with

FIGURE 23. Dynamic Sensitivities of X, Y, and Z with respect to the Mathematical Parameter A for the Human (——) Squirrel Monkey (° ° °), Rat (- - -), and Mouse (— —).

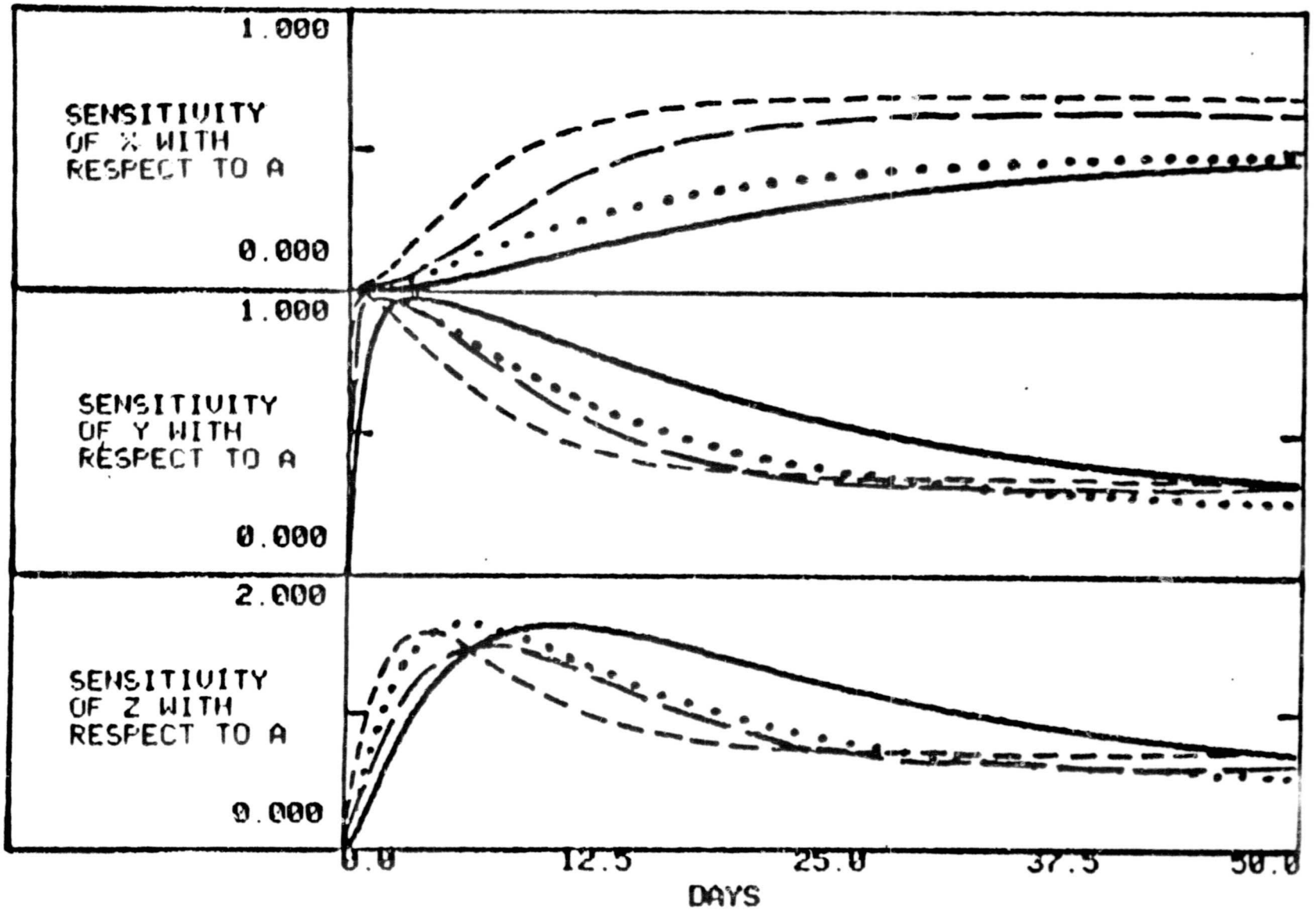

FIGURE 24. Dynamic Sensitivities of X, Y, and Z with respect to the Mathematical Parameter C for the Human (——), Squirrel Monkey (° ° °), Rat (- - -), and Mouse (— —).

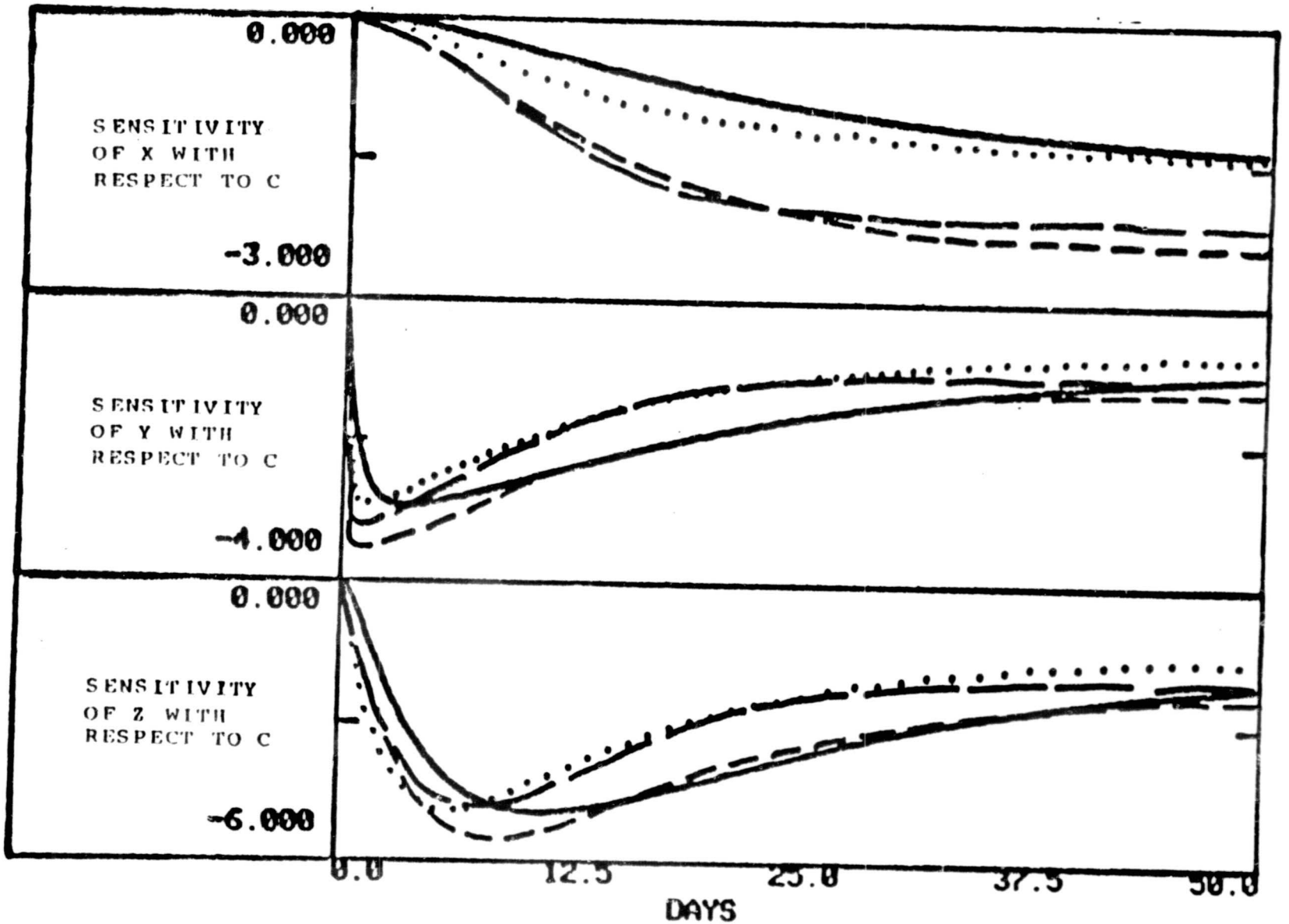

FIGURE 25. Dynamic Sensitivities of X, Y, and Z with respect to the Mathematical Parameter A for the Human (——), Squirrel Monkey (° ° °), Rat (- - -), and Mouse (— —).

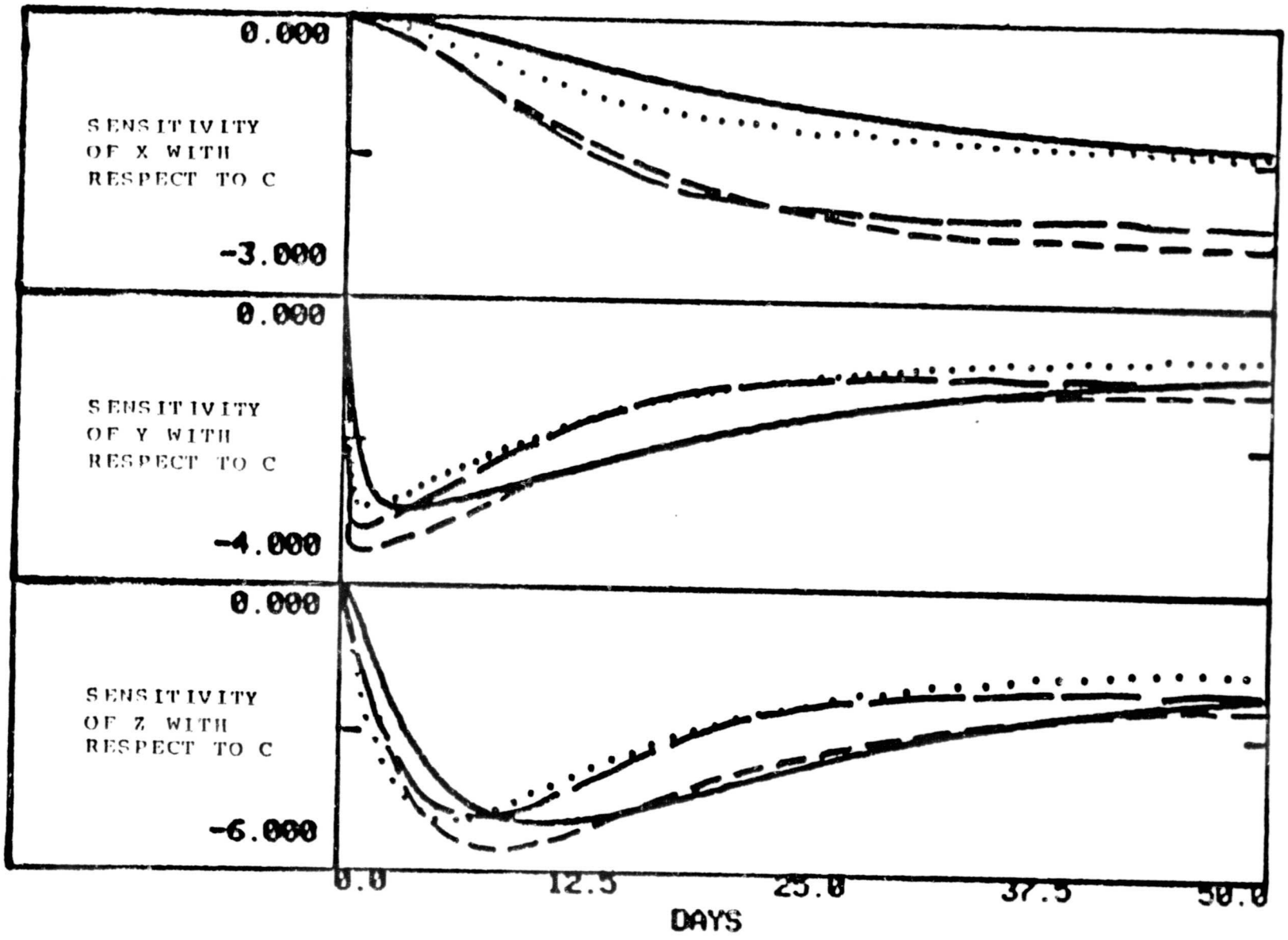

FIGURE 26. Dynamic Sensitivities of X, Y, and Z with respect to the Mathematical Parameter C for the Human (-----), Squirrel Monkey (• ° °), Rat (- - -), and Mouse (-- --)

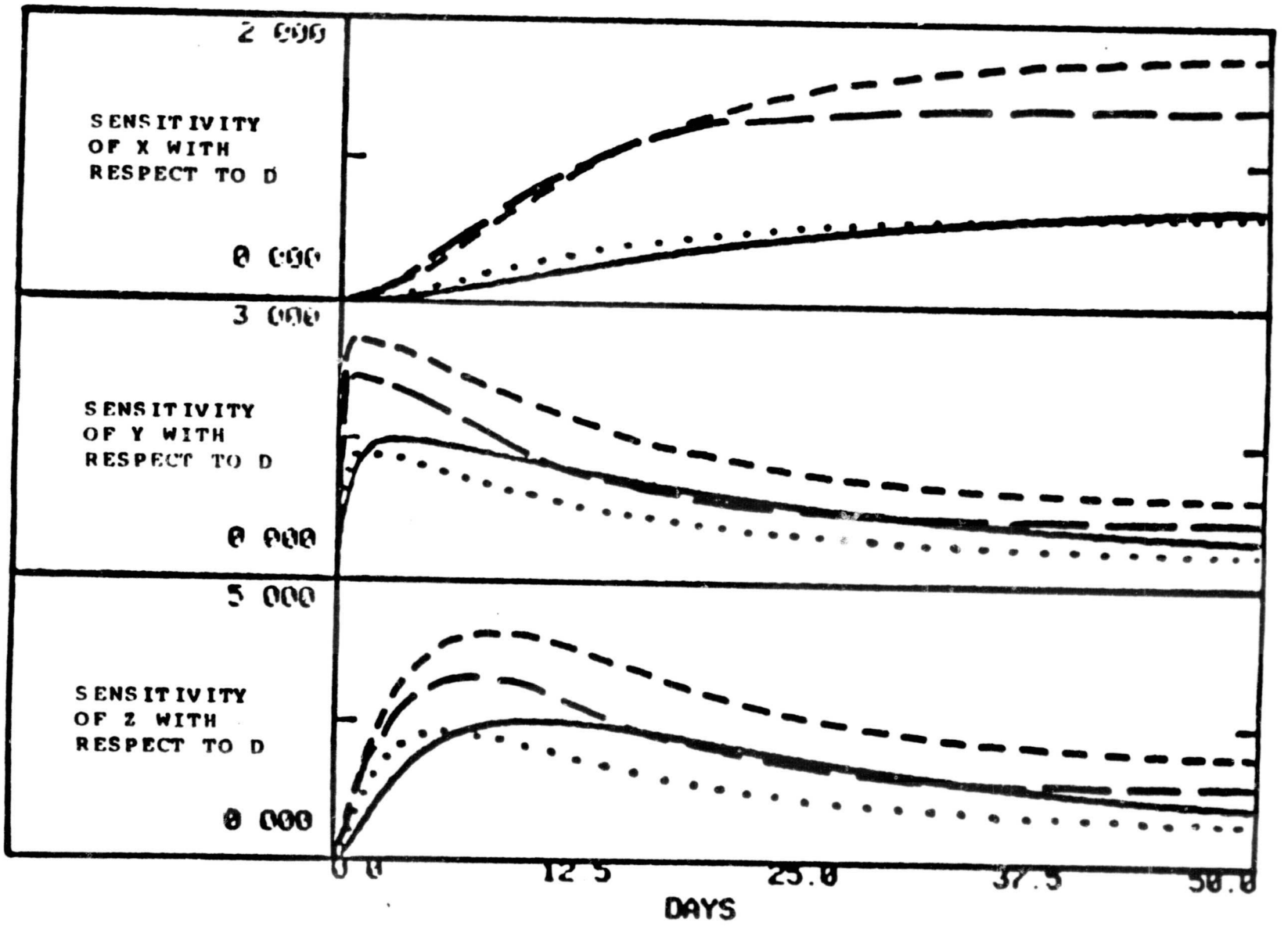

Figure 27. Dynamic Sensitivities of X with respect to the Physiological Parameters P50, PAO, PV, Q, and VM for the Human (——) Squirrel Monkey (° ° °), Rat (- - -) and Mouse (— —).

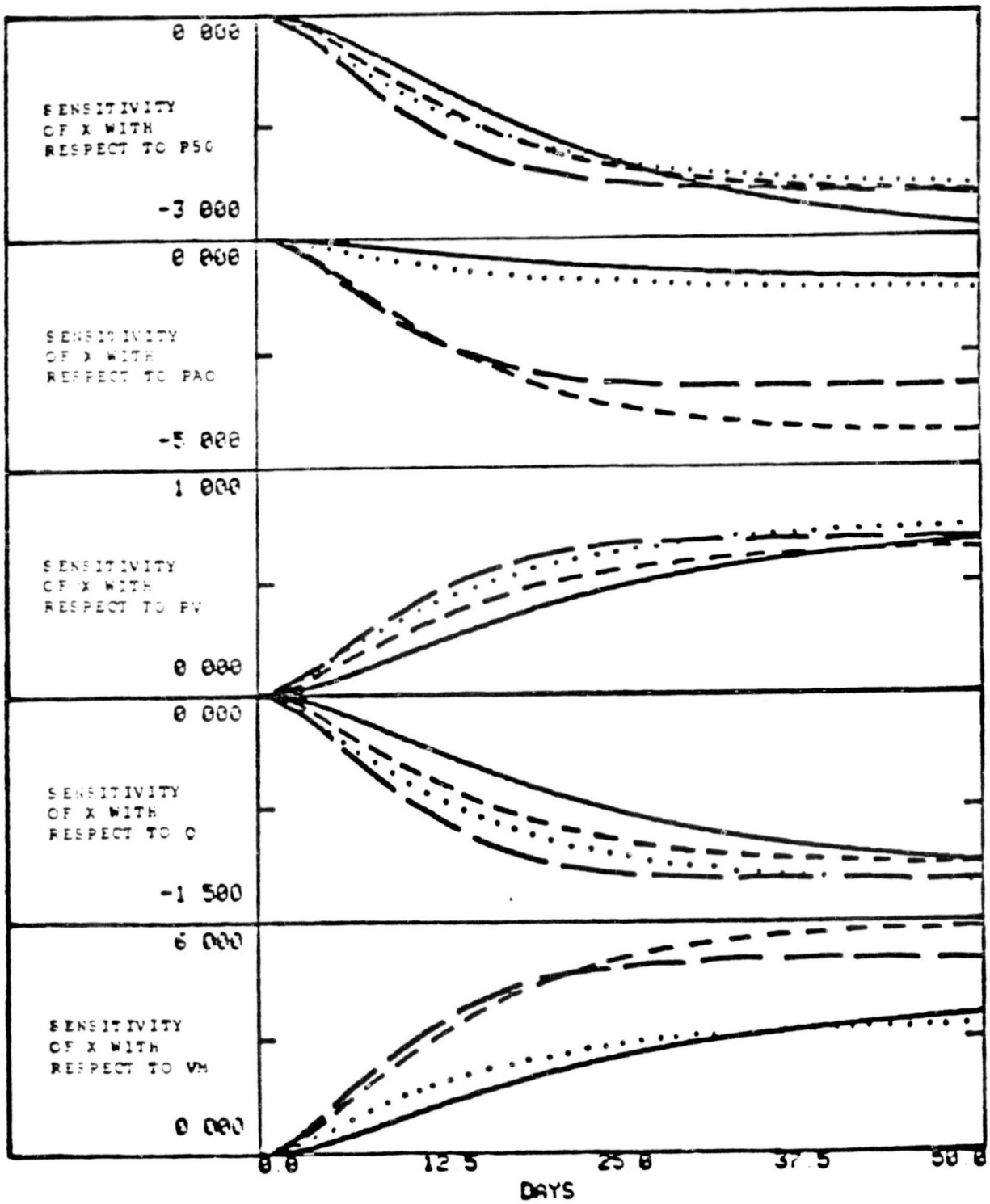

Figure 28. Dynamic Sensitivities of Y with respect to the Physiological Parameters P50, PAO, PV, Q, and VM for the Human (——), Squirrel Monkey (° ° °), Rat (- - -), and Mouse (— —).

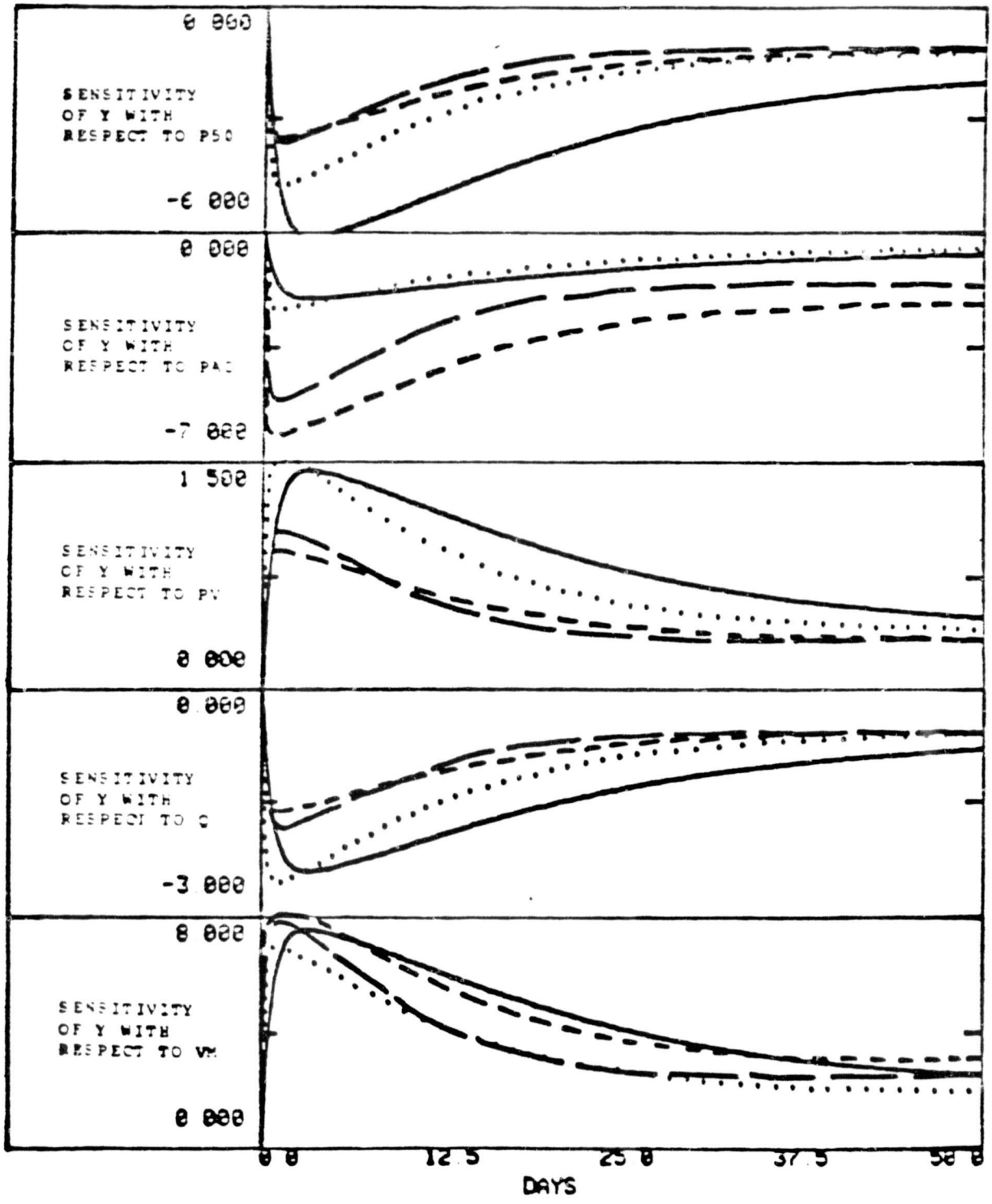

Figure 29. Dynamic Sensitivities of Z with respect to the Physiological Parameters P50, PAO, PV, Q, and VM for the Human (——), Squirrel Monkey (° ° °), Rat (- - -), and Mouse (— —).

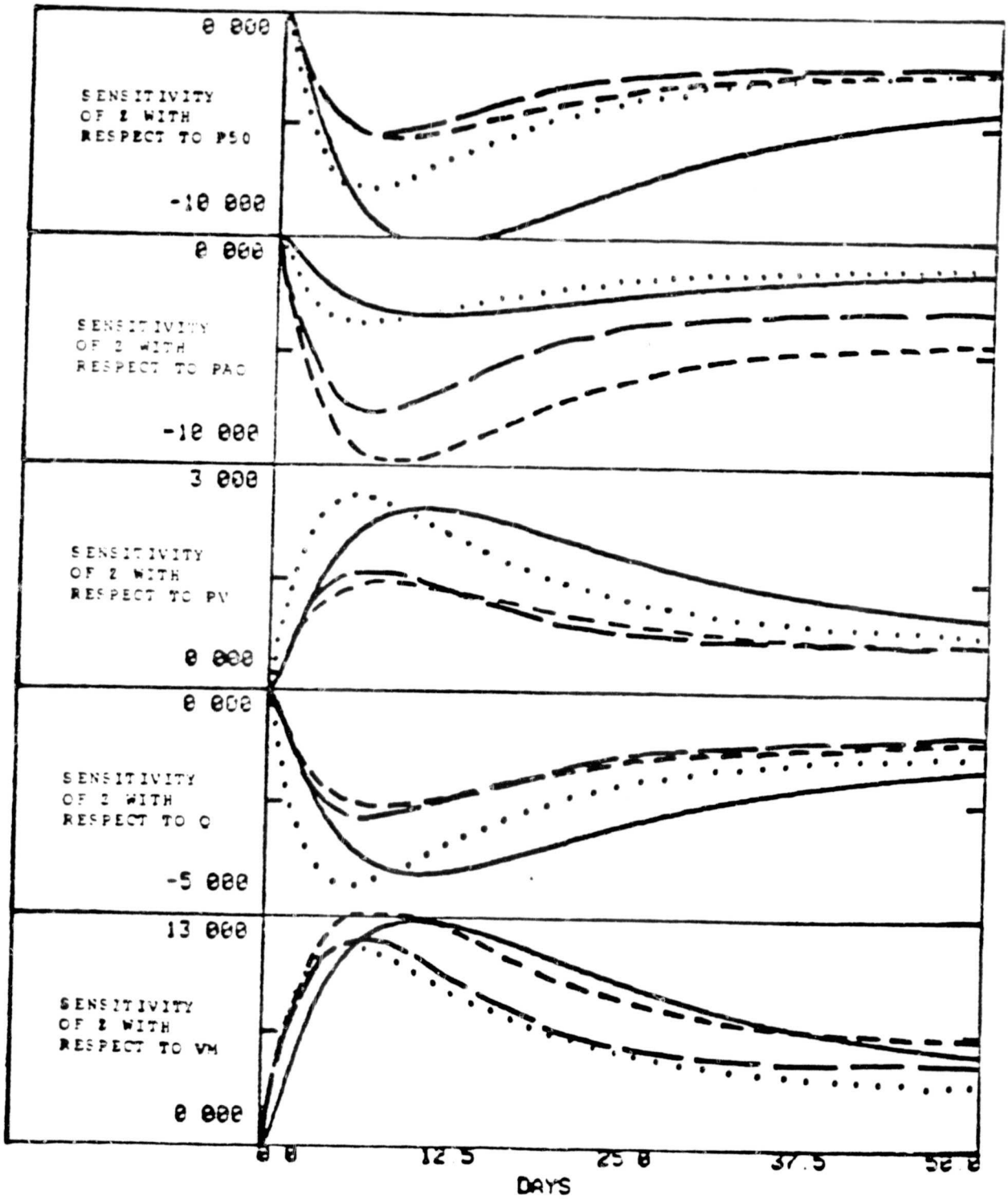

the equations for X, Y, and Z. For all species, the values of K1 are at least an order of magnitude smaller than the values of K2 and K3 (see Table 3). Values of the parameter K3 are within the same order of magnitude as K2 values, but are consistently smaller. The three constants correspond to the time frames associated with the physiology of the three variables, X, Y, and Z. Changes in variable Y, erythropoietin concentration, can take place within a few hours (K2); changes in Z, red blood cell production, occur within a few days (K3); while changes in X, red cell mass, only begin to take place after many days (K_1).

No consistent patterns were discovered to link the dynamic sensitivities between species except for the sequence in which the curves for a given parameter would peak in value. These sequences always followed the ranking of the individual time constants between species. For example, in Figure 23 the third set of curves represent the dynamic sensitivities of Z with respect to A. The sequence in which these four curves peak in value is directly related to the species specific values of K3 (see Table 3). Table 9 presents a ranking of the constants K1, K2, and K3 for all four species with a numerical value of 1 being given to the shortest values and a 4 to the longest values.

3.2 SIMULATED STRESSES

The second half of the species comparison study of the erythropoiesis control system involved a series of comparative simulations performed using the four species specific models. These simulations were performed in order to study the species-to-species (between species) response to the following stresses: Long-term hypoxic exposure and recovery, red cell infusion, loss of red cell mass, and plasma volume depletion. For each of these simulations, the two gain factors in the model, G1 (the gain of the erythropoietin control function) and G2 (the gain of the marrow red blood cell production-control function), were held constant in order to examine how the known differences in physiological parameters values between species affect model operation.

Table 9. Numerical Ranking of the Time Constants K1, K2, and K3

Species	K1	K2	K3
Man	1	1	1
Squirrel Monkey	2	3	4
Rat	3	4	2
Mouse	4	2	2

3.2.1 Long-Term Hypoxic Exposure and Recovery

One environmental stress that is typically used to study the erythropoietic system is altitude hypoxia and descent from altitude (recovery). In order to determine how the four species models respond to these two stresses, the following simulation was performed using each of the models. First, the model was run for 10 days to provide baseline control data, the arterial oxygen tension level (P_aO) was then decreased by 10 percent and the model run for 100 days to simulate long-term exposure to altitude hypoxia. P_aO was then returned to its normal (sea level) value and the model run for an additional 100 days to simulate descent from altitude (recovery). Even though this may be a simplistic way of simulating the effects of hypoxia on the erythropoietic system, the comparison between models should still be valid (unless there is a species difference in the process of altitude adaptation), since all four models were exposed to the same relative stresses. Altitude adaptation involves more than a simple change in red cell mass in response to the decrease in P_aO. The adaptation process typically includes an increase in pulmonary ventilation, a change in P_{50}, a change in oxygen diffusing capacity, and an increase in whole-body vascularity.

Figure 30 shows the results of this simulation on a selected subset of model variables for all four species. The values for the variables have been scaled to represent changes from normal (that is, pre-stressed levels are equal to 1.0).

All four species models show a qualitatively similar response to the step decrease in P_aO (altitude hypoxia) and the step increase in P_aO back to the original value (recovery from altitude). In the model, the decrease in arterial oxygen tension causes the oxygen balance at the kidney to be changed, this change is sensed by renal tissues sensitive to oxygen tension levels, and results in an increase in erythropoietin release which in turn increases red cell production (RCP). With this increase in RCP, red cell mass (RCM) and hematocrit (HCT) increase slowly over time until a new balance between RCP and red cell destruction (RCD) is reached and all of the variables reach a new "adapted" steady-state. During descent from altitude (recovery), essentially the reverse procedure as described above takes place. At the end of 100 days

Figure 30. Simulation of Long Term Exposure to 10% Hypoxia and Recovery from Hypoxia in Man (———), Squirrel Monkey (° ° °), Rat (- - -), and Mouse (— —).

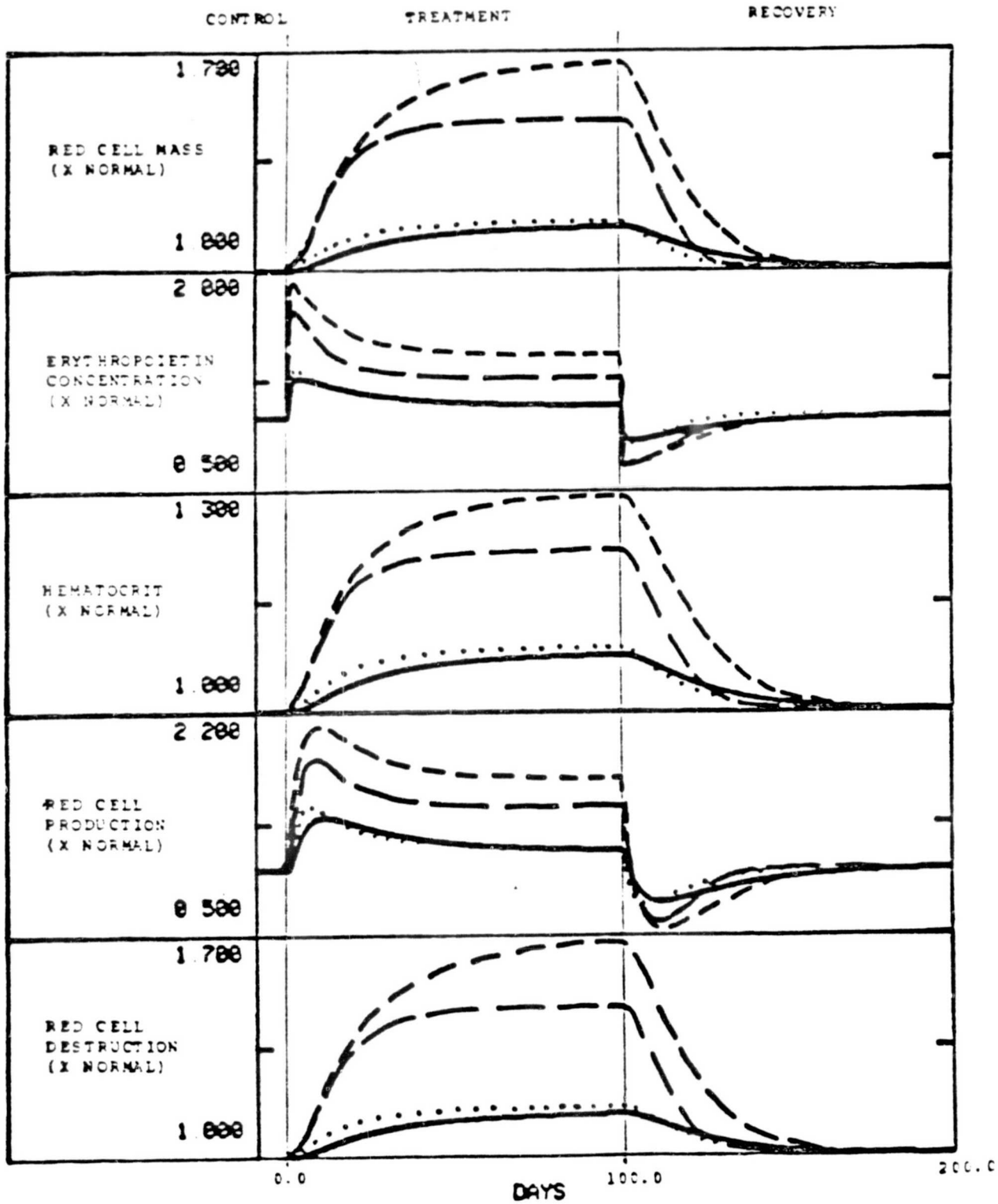

the model has "adapted" to the hypoxic state, returning the P_aO to normal is equivalent to increasing P_aO in a sea level adapted model. This relative increase in P_aO I is interpreted by the renal oxygen tension sensor in the model as a positive oxygen balance and decreases erythropoietin production and concentration. The decrease in erythropoietin concentration brings about a corresponding decrease in RCP. Over time, the decreased RCP causes the Red Cell Mass (RCM) and hematocrit to slowly return to the normal sea level values.

While the species response to these two stresses are qualitatively the same, the responses (model) differ in two fundamentally different ways. First, there are species differences in the amplitudes of the response to the stress. The rat and mouse models show a much more marked response to changes in P_aO than do the human and squirrel monkey models. For example, in response to a 10 percent decrease in P_aO, RCM is predicted by the rat and mouse models to increase by 50 to 70 percent, while in the human and squirrel monkey models RCM increases only 14 to 15 percent for the same percent reduction (this agrees with the steady state sensitivities and ranking of steady state sensitivities shown in Tables 4 and 7). The second difference involves how quickly each model responds to the stresses. For example, RCM reaches the new steady-state value (adapted value) in the mouse and squirrel monkey approximately 50 days following exposure to hypoxia while the rat and human models are just reaching steady-state after 100 days. These differences are associated with the inter-species differences in the time constants (see Tables 3 and 9).

3.2.2 Red Cell Infusion/Red Cell Loss

Two additional and closely related stresses that were studied with respect to interspecies differences were an acute increase in red cell mass (red cell infusion) and an acute decrease in red cell mass (blood loss). The response of the models to a simulated 10 percent increase in red cell mass is shown in Figure 31, while the model response to a sudden 10 percent decrease in red cell mass is shown in Figure 32. In these simulations, the response of the mode to the two stresses are identical if the direction of change about the normal operating point is ignored (that is, the absolute value of the of the percent change from normal is identical for the two stresses for any given

Figure 31. Simulation of a 10 percent RCM Infusion in Man (———), Squirrel Monkey (° ° °), Rat (- - -), and Mouse (— —).

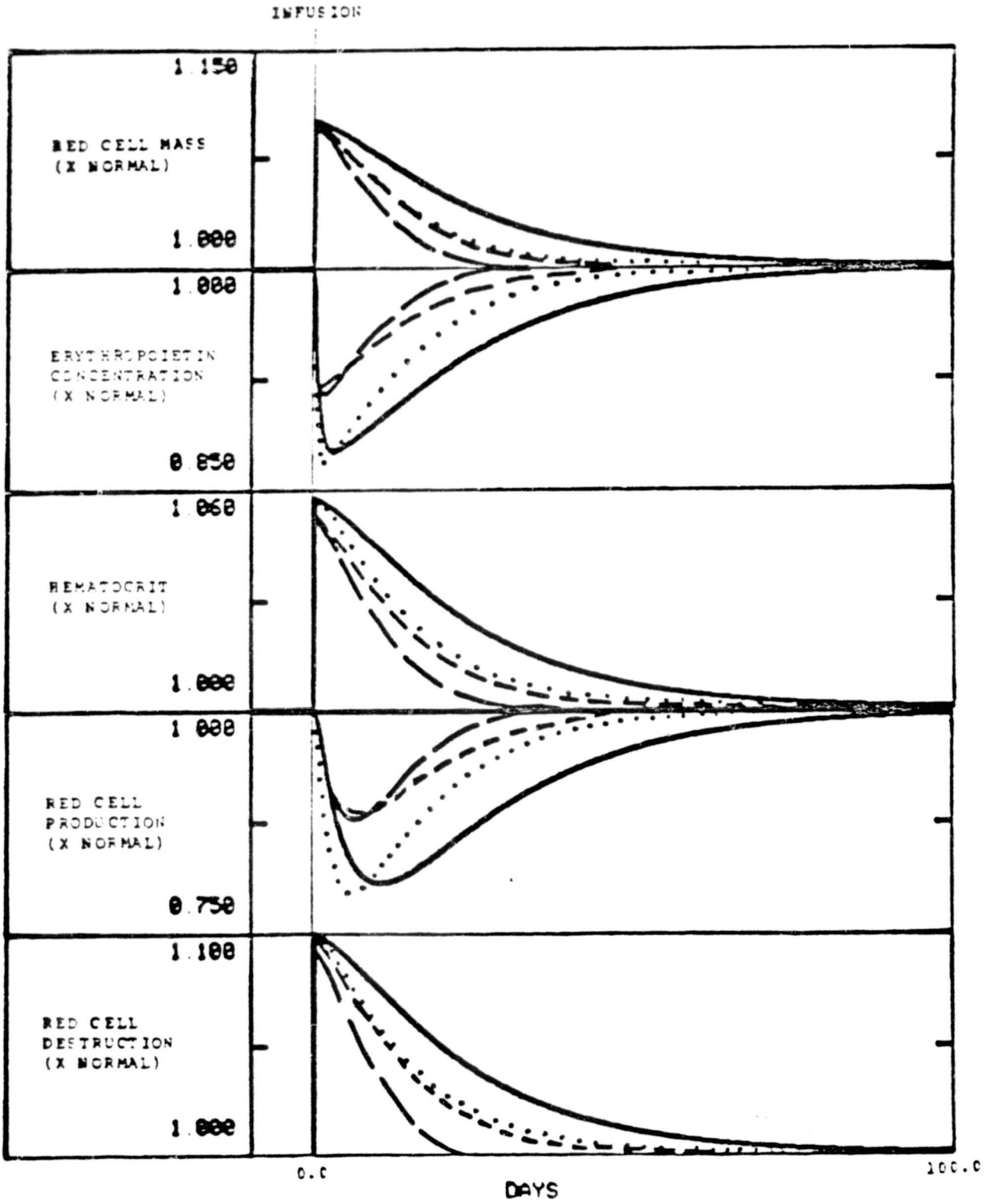

Figure 32. Simulation of a 10 percent RCM Loss in Man (——), Squirrel Monkey (° ° °), Rat (- - -), and Mouse (— —).

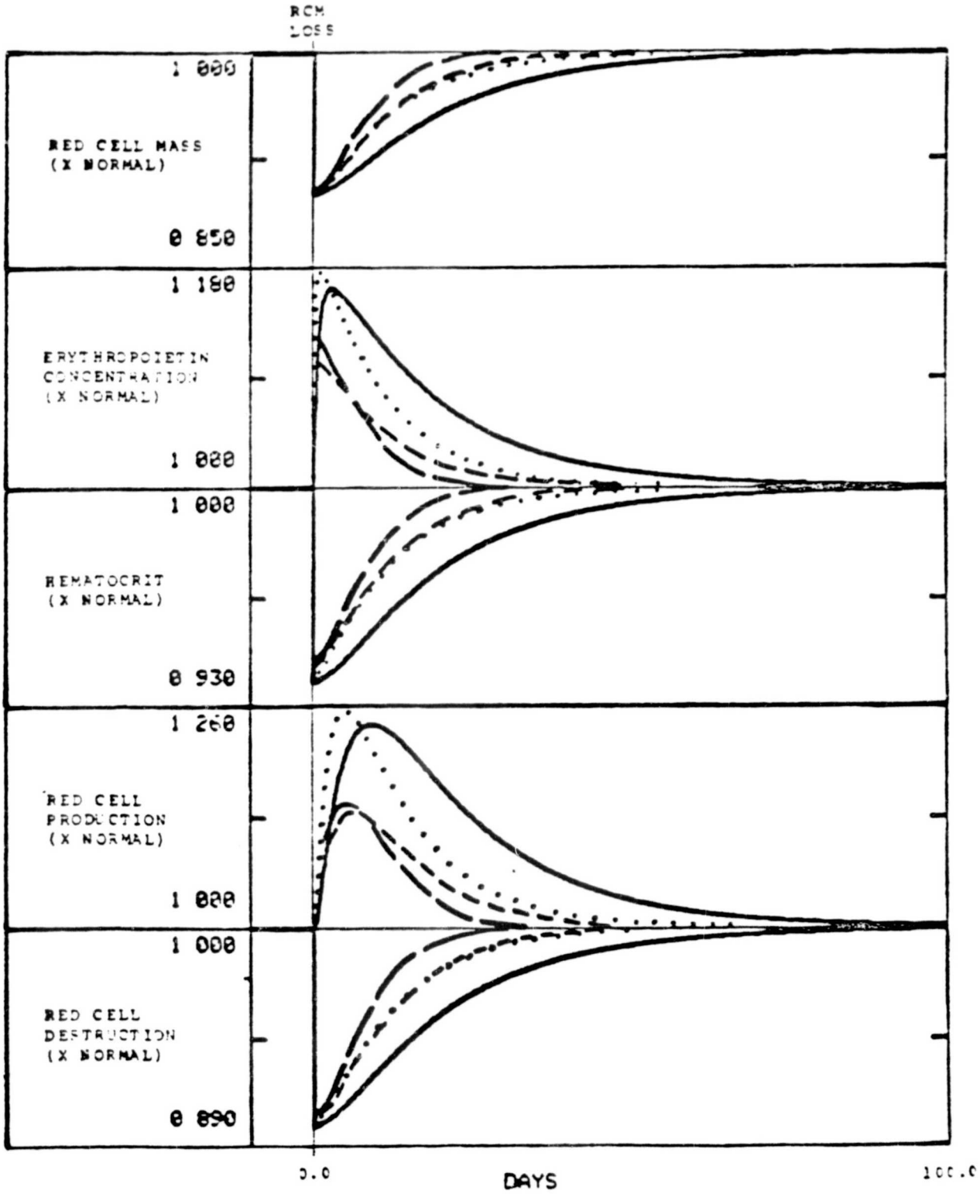

species). A comparison of Figures 31 and 32 show that an infusion of red blood cells causes the model to respond in a nearly opposite fashion to a red cell loss for all species. For this reason, this discussion has been limited to only one of the stresses, red cell loss (the other stress causes the opposite senario to take place). The decrease in red cell mass caused by the loss causes a decrease in the oxygen supplied to the kidney (renal tissues sensitive to oxygen balance). This decrease causes an in balance of oxygen at the renal oxygen sensor and renal oxygen tissue tension decreases. This decrease results in the increased production of erythropoietin and the corresponding increase in red cell production. As red cell mass increases back towards normal, the oxygen balance at the renal oxygen sensor returns towards normal and erythropoietin production drops accordingly until the system returns to normal (that is until the red cell mass returns to it normal value).

By examining the species results for red cell production following a 10 percent artificial decrease in red cell mass, two types of interspecies differences exist. First, there is the magnitude of the responses, and second there is how quickly the model responds to the stress and consequently, how quickly the model reaches a new steady-state. The magnitude of the response is related to the steady-state sensitivity of the model to changes in the normal value of red cell mass, RCM0, with man and squirrel monkey being more sensitive to the blood loss than the rat and mouse. The frequency (or "quickness") with which the model reacts to the blood loss is related to the three time constants K1, K2, K3. For red cell production, the time constant of interest is K3. Based on the senstivity values in Table 2, it would be predicted that the mouse model would respond most quickly to a blood loss followed by the rat, squirrel monkey, and human. This predicted result was shown to be true in Figure 31.

3.2.3 Erythropoietin Infusion

An interesting experiment to perform (if it were possible) would be to study the effect that injections of erythropoietin would have on the control of erythopoiesis and how the effect varies between species. In order to study how the four species models respond to step increases in erythropoietin

concentration, the following simulation was performed using each of the models. The model was run for 10 days to generate simulated control data. A stress equivalent to a 10 times normal injection of erythropoietin was then applied to the model. The model was run for 100 days in order to show the species response to the stress. The results of this simulation for all four species is shown in Figure 33. All four species showed the same qualitative response to the erythropoietin injection. In the model the increased erythropoietin caused a corresponding increase in red cell production which causes an increase in red cell mass. As the injected erythropoietin is metabolized (see erythropoietin half life, $TE_{1/2}$, in Table 2), the erythropoietin concentration and red cell production decreases to below normal since red cell mass (the controlled variable) has increased to above normal (due to the increased erythrpoietin concentration). Erythropoietin and red cell production then gradually increase back towards normal as redcell mass decreases down to normal. The species difference in the magnitude of the model response to the erythropoietin injection is related to the species differences in sensitivities to changes in E_0 with the human being most sensitive and the squirrel monkey, rat, and mouse producing approximately the same magnitude of response. The rate of the model response to the stress is related to the species difference for the time constants K1, K2, and K3 respectively (see Table 5). In all cases, the human responded the slowest and the general trend was for the response to decrease as the body mass of the animal decreased (see Table 7).

3.2.4 Plasma Volume Depletion

Plasma volume depletion has been used previously with the human model to simulate the effects of space flight on the erythropoiesis system. In order to study the species response and to compare the use of the squirrel monkey, rat, and mouse as analogs of human erythropoiesis control during space flight, plasma volume depletion simulations were performed for the human, squirrel monkey, rat, and mouse. The simulations consisted of seven days of control, followed by 7 days of plasma volume depletion, which in turn was followed by 14 days of recovery. These time periods were selected as being representative of a one-week Spacelab mission. The plasma volume was decreased by 10 percent for each species the first inflight day, held at this level for seven days,

Figure 33. Simulation of a 10 X Normal Erythropoietin Infusion in Man (——) Squirrel Monkey (° ° °), Rat (- - -), and Mouse (— —).

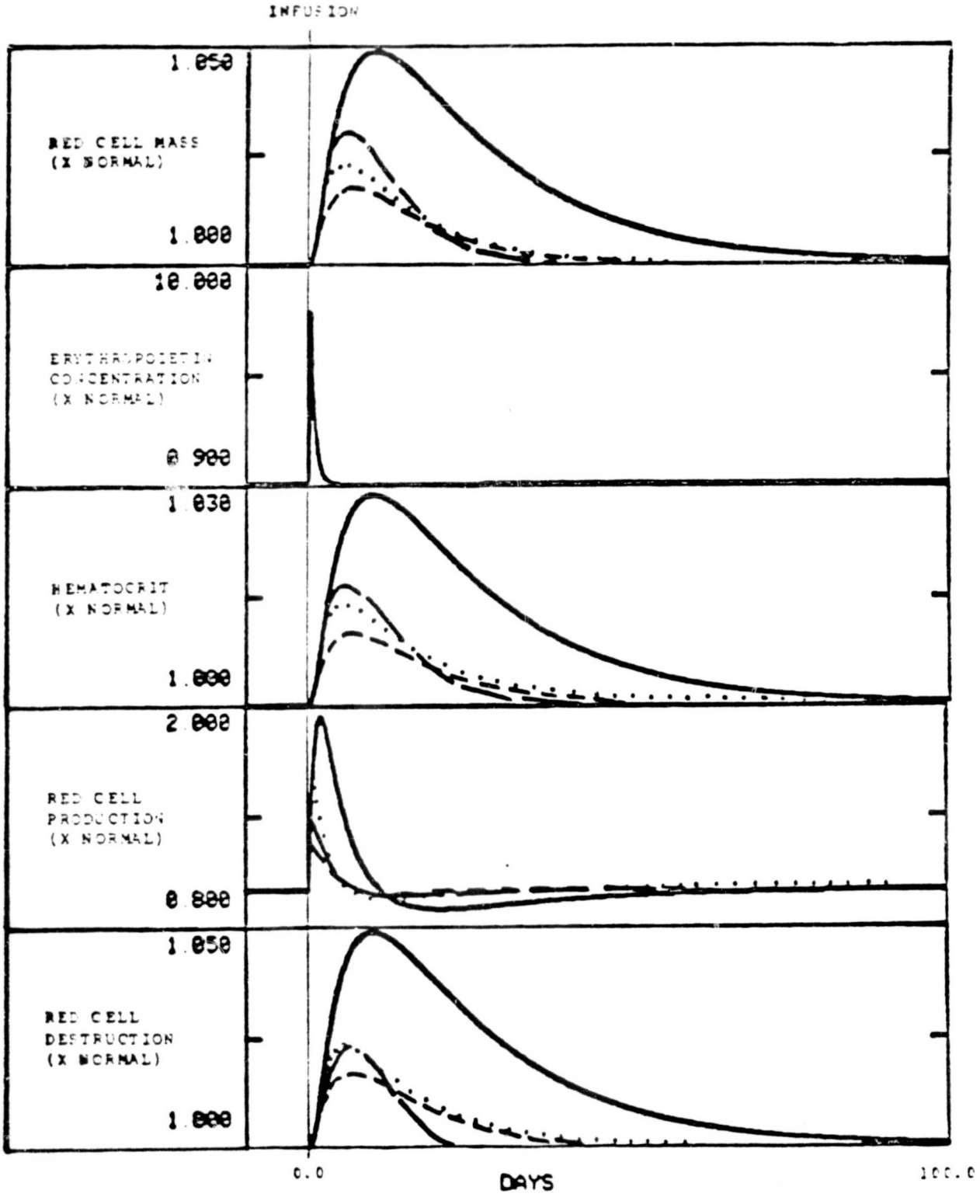

then returned to normal at the end of the seventh day. Figure 34 shows the results of this simulation for all four species. The data shown represent a selected set of hematological variables for each species. The values for the variables shown in Figure 34 have been scaled to represent changes from normal.

The qualitative response of all four species to a 10 percent decrease in plasma volume is approximately the same. All four show gradual decreases in red cell mass and red blood cell destruction, along with more dramatic decreases in erythropoietin concentration and red blood cell production during the treatment phase. These decreases are all caused by the increase in hematocrit which in turn is due to the plasma volume depletion. The species differences that are observed have to do with the magnitude and the rate at which the changes take place. As can be seen, there is no uniform ranking between the species as to how they respond to the stress for each of the variables. This is due to the fact that for the selected combination of parameters for each species there no consistent ranking between species for the steady-state sensitivities (magnitude of response, see Table 5), or for the time constants (rate of responses, see Table 3). However, the simulations do show that the qualitative response to the stress is consistent between the species; that is, the variable values respond in a similar fashion for all four species.

Figure 34. Simulation of a 7 day 10 percent Plasma Volume Depletion in Man (——) Squirrel Monkey (° ° °), Rat (- - -) and Mouse (— —).

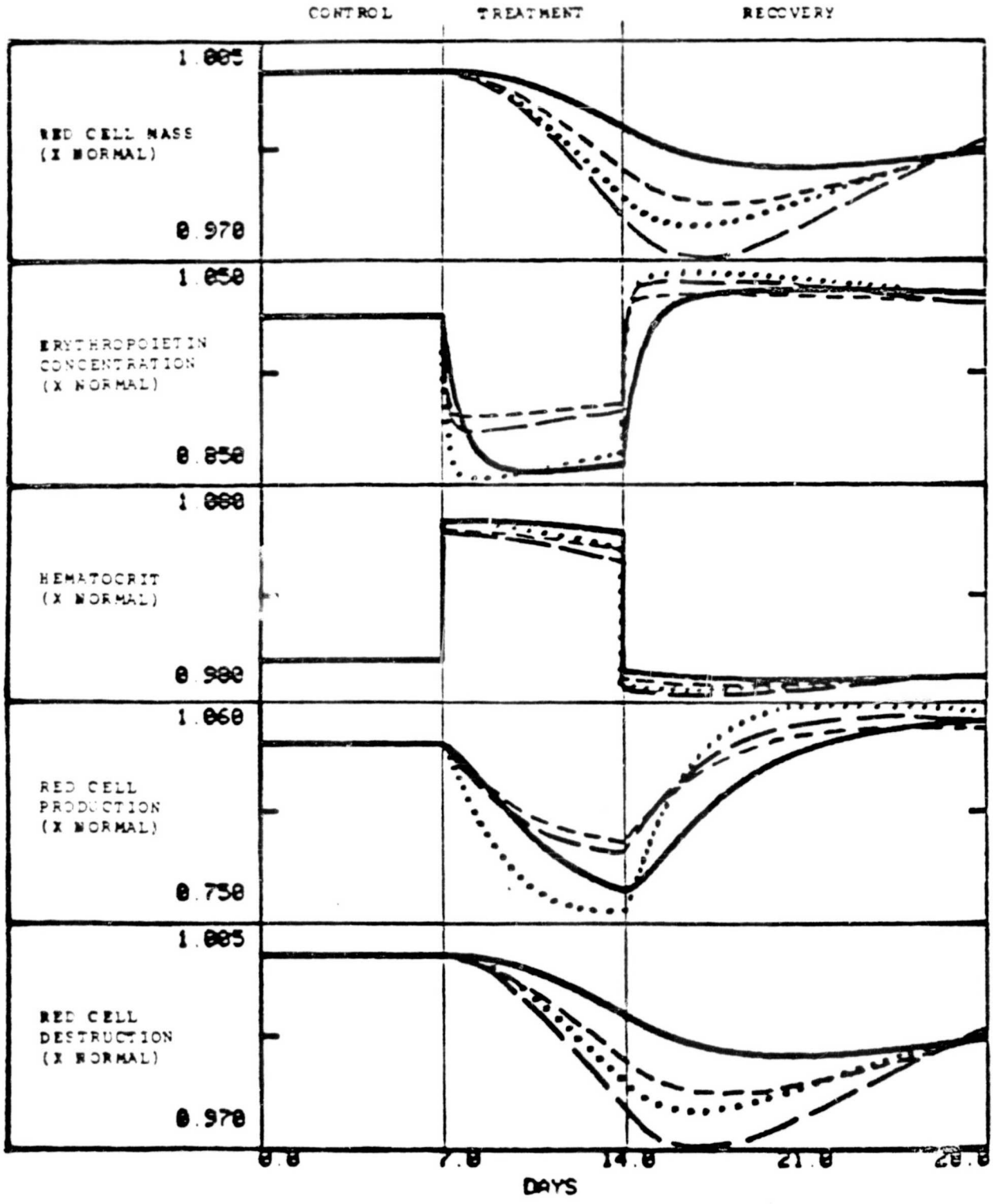

4.0 DISCUSSION

This appears to be the first time that a single model formulation has been used to represent (model) the same physiological system for several different species. In the past, parameter values and experimental erythropoietic data from one animal species have been used to validate models and to estimate model parameters for other species, but they have not previously been used to develop separate species specific models for the same physiological system. The approach presented in this paper for creating species specific models is based on the assumption that the basic concept of erythropoiesis control is identical among the species of interest. The overall model formulation described in the first part of the paper is general and it is assumed that the erythropoiesis control system for all four species is identical. This does not necessarily imply that either the detailed physiology or the anatomical correspondence between species is identical. For example, in the model, all of the hemopoietic tissue is grouped into one compartment. This one compartment, however, may be anatomically equivalent to several different organs. In man, this compartment is equivalent to active bone marrow, while in the mouse this compartment may consist of two or more anatomical components (bone marrow, spleen, etc.).

The significance of being able to simulate several different species using the same general model description is that, while there may be anatomical differences, the physiologies are governed by the same factors. This implies that one species can be used to study the physiology of another species. The differences between the response of two different species to erythropoietic stresses may be due to differences in operating points rather rather than differences in physiological control mechanisms. An example of this is shown in Figure 22, where each species has significantly different arterial oxy-hemoglobin saturations, due to inherent (species dependent) differences in arterial oxygen tension and P50. The location of the normal operating point for the model on the non-linear oxy-hemoglobin dissociation curve can cause two species with the same control mechanisms to respond to stresses in significantly different ways. For example, a small decrease in P_aO in the human will cause arterial saturation to decrease slighty and will have very little impact on model operation while the same percent decrease in arterial

oxygen tension in the mouse will cause a more dramatic change in saturation and a corresopndingly larger impact on model operation. This is due to the fact that the normal operating point for the mouse is lower on the dissociation curve and a change in arterial oxygen tension will drop the new operating point down into the nonlinear portion of the curve where saturation values decrease rapidly as arterial oxygen tension decreases.

While there are differences in the simulation results between species, all four models respond qualitatively the same to the simulated stresses that have been applied. Any differences were accounted for by either species differences in operating points on the oxy-hemoglobin dissociation curve (see Figure 22), or differences in the time constants.

The overall results of this study are encouraging, for they show that there is promise in using the same model formulation, to study the response of several different species to erthropoietic stresses. However, caution must be taken at this point in time due to the lack of experimental data with which to completely validate the squirrel monkey and rat version of the model. The most ideal set of experimental data would be the collection of data from all four species under identical experimental conditions, thus providing not only validation data, but additional data as to the nature of the species differences in erythropoietin regulation.

This computer simulation study demonstrates the utility of performing sensitivity analyses in conjunction with model formulation. They clearly demonstrate the role and importance of parameter values in interpreting and understanding the functioning of the model and in helping to analyze the physiology of a given system as is currently understood.

5.0 REFERENCES

1. Leonard, J.I., Kimzey, S.L., and Dunn, C.D.R. Dynamic Regulation of Erythropoiesis: A Computer Model of General Applicability. Exp. Hematol., 9(4):355-78, 1981.

2. Dunn, C.D.R., Leonard, J.I., and Kimzey, S.L. Interactions of Animal and Computer Models in Investigations of the "Anemia" of Space Flight. Aviat. Space Environ. Med. 52(11):683-90, 1981.

3. Nordheim, A.W., White, R.J., and Leonard, J.I. Analysis of a Twelve-Parameter Non-Linear Model of Erythropoiesis. Proceedings of the 1982 Summer Computer Simulation Conference, Simulation Councils, Inc., La Jolla, 64-70, 1982.

4. Nordheim, A.W., White, R.J. and Leonard, J.I. Analysis of a Twelve-Parameter Non-Linear Model of Erythropoiesis. TIR 2114-MED-2009, Management and Technical Services Company, Houston, TX, 1981.

5. Stahl, D. System Parameters for the Species-Independent Model of Erythropoiesis Control: A Species Comparison of Normal Values in the Human, Squirrel Monkey, Rat, and Mouse Models. TIR 2114-MED-2010, Management and Technical Services Company, Houston, TX, 1981.

6. Neal, L. A Numerical Method for Solutions of Systems of Stiff Differential Equations: The Hybrid Euler Integration Technique. TIR 741-LSP-9016, General Electric Company, Houston, TX, 1979.

7. Neal, L. A Fast Variable Step Size Integration Algorithm for Computer Simulations of Physiological Systems, TIR 2114-MED-1005, Management and Technical Services Company, Houston, TX, 1981.

8. Buderer, M.C. and Pace, N. Hemopoiesis in the Pig-Tailed Monkey Macaca Nemestrina During Chronic Altitude Exposure. Am. J. Physiol. 223(2):346-52, 1972.

9. Torrance, J.D., Lenfant, C., Cruz, J., and Marticorena, E. Oxygen Transport Mechanisms in Residents at High Altitude. Respirat. Physiol. 11, 1-15, 1970/71.

10. Weil, J.V., Jamieson, G., Brown, D.W., and Grover, R.F. The Red Cell Mass - Arterial Oxygen Relationship in Normal Man. J. Clin. Invest., 47, 1627-39, 1968.

11. Winslow, R.M., Monge, C.C., Statham, N.J., Gibson, C.G., Charache, S., Whittenbury, J., Morgan, O., and Berger, R.I. Variability of Oxygen Affinity of Blood: Human Subjects Native to High Altitude. J. Appl. Physiol: Respirat. Environ. Exercise Physiol. 51(6):1411-16, 1981.

12. Pepelko, W.F. Effect of Hypoxia and Hypercapnia Alone and In Combination Upon the Circulating Red Cell Volume of Rats. Proc. Soc. Expt. Biol. and Med. 136, 967-71, 1971.

13. Mylrea, K.C. An Investigation of the Erythropoietic Response of Mice to Hypoxia and a Mouse Model for the Control of Erythropoesis. Ph.D. Thesis, University of Michigan, 1968.

APPENDIX A

ANALYTICAL DERIVATION OF STEADY-STATE SENSITIVITIES FOR ERYTHROPOIESIS MODEL

I. The sensitivity coefficient of the dependent variable, V, with respect to the independent variable, p is defined as

$$\frac{\partial V}{\partial p} \sim \quad \text{Sensitivity Coefficient}$$

$$\Delta V = \Delta p \left(\frac{\partial V}{\partial p}\right)$$

normalized version

$$\frac{\Delta V}{V_o} = \frac{\Delta p}{P_o} \left(\frac{P_o}{V_o} \quad \frac{\partial V}{\partial p} \right)$$

Let the sensitivity of V with respect to p , , be defined as

$$S_p^V = \frac{P_o}{V_o} \left(\frac{\partial V}{\partial p}\right)_o .$$

Note: for the normalized model, $V_o = 1$,

$$S_p^V = P_o \left(\frac{\partial V}{\partial p}\right)_o . \qquad (1)$$

II. To determine the steady-state sensitivities, $\left(\frac{\partial V}{\partial p}\right)_c$ must be calculated.

Recall from the main text of this paper that in the steady-state

$X = F_3(y)$ and

$y = F_2(x)$

$z = X$

where $F_3(y) = \begin{cases} y^{G_2}, & y < 1 \\ 1 + G_2 \log(y), & 1 \le y \le e^{4/G_2} \\ 6 - e^{G_2 \exp\left(-G_2 \cdot y \cdot e^{-4/G_2}\right)}, & y > e^{4/G_2} \end{cases}$

and $F_2(x) = A \exp\left[- B \cdot W^n\right]$, $W = \frac{CX-1}{DX+1}$

It can be shown that $\left(\frac{\partial V}{\partial p}\right)$ for the dependent variable x and y

$$\left(\frac{\partial X}{\partial p}\right) = \frac{\left(\frac{\partial F_3}{\partial p}\right)_y + \left(\frac{\partial F_3}{\partial p}\right)_p \left(\frac{\partial F_2}{\partial p}\right)_x}{1 - \left(\frac{\partial F_3(y)}{\partial y}\right)_p \left(\frac{\partial F_2(X)}{\partial x}\right)_p} \qquad (2)$$

$$\left(\frac{\partial y}{\partial p}\right) = \left(\frac{\partial F_2}{\partial p}\right)_x + \left(\frac{\partial F_2}{\partial x}\right)_p \left(\frac{\partial X}{\partial p}\right), \quad \text{and} \qquad (3)$$

$$\left(\frac{\partial Z}{\partial p}\right) = \left(\frac{\partial X}{\partial p}\right). \tag{4}$$

Where, about the normal operating point of $y_o = y = 1$

$$\left(\frac{\partial F_3}{\partial y}\right)_p = \frac{G_2}{y} = G_2$$

$$\left(\frac{\partial F_3}{\partial p}\right)_y = \log y = \log(1) = 0 \quad , \quad \text{for } p = G_2$$

$$\left(\frac{\partial F_3}{\partial p}\right)_y = 0 \quad , \quad \text{for } p \neq G_2$$

$$\left(\frac{\partial F_2}{\partial X}\right)_p = \frac{-n \cdot B \cdot (C+D)}{(DX+1)^2} \cdot W^{n-1} \cdot F_2(X) \tag{5}$$

$\left(\frac{\partial F_2}{\partial p}\right)$ for the mathematical parameters A, B, C, D, and n are as follows:

$$\frac{\partial F_2}{\partial A} = \frac{F_2(X)}{A} \tag{6}$$

$$\frac{\partial F_2}{\partial B} = -W^n \cdot F_2(X) \tag{7}$$

$$\frac{\partial F_2}{\partial C} = \frac{-n \cdot B \cdot X}{(DX+1)} \cdot W^{n-1} \cdot F_2(X) \tag{8}$$

$$\frac{\partial F_2}{\partial D} = \frac{n \cdot B \cdot X}{(DX+1)} \cdot W^n \cdot F_2(X) \quad \text{and} \tag{9}$$

$$\frac{\partial F}{\partial n} = -B \cdot W^n \cdot F_2(X) \log(W). \tag{10}$$

About the normalized operating point, $x_o = y_o = z_o = 1$, the following statements are true:

$$\left(\frac{\partial F_3}{\partial y}\right)_o = G_2 \ , \quad F_2(1) = 1 \ , \quad F_3(1) = 1, \text{ and}$$

$$\left(\frac{\partial F_2}{\partial X}\right)_o = \frac{-n \cdot B \cdot (C+D)}{(D+1)^2} \cdot W(1)^{n-1} \quad , \quad W(1) = \frac{C-1}{D+1}$$

Therefore, $\left(\frac{\partial V}{\partial p}\right)$ for V = X and Y , and p = A, B, C, D, or n (that is, equations 2, 3, and 4) become

$$\left(\frac{\partial X}{\partial p}\right)_o = \frac{G_2}{1 - G_2 \left(\frac{\partial F_2}{\partial X}\right)_o} \cdot \left(\frac{\partial F_2}{\partial p}\right)_o,$$

$$\left(\frac{\partial y}{\partial p}\right)_o = \frac{1}{G_2} \left(\frac{\partial X}{\partial p}\right)_o \quad , \text{ and}$$

$$\left(\frac{\partial Z}{\partial p}\right)_o = \left(\frac{\partial X}{\partial p}\right)_o$$

when $\left(\frac{\partial F_2}{\partial p}\right)$ and $\left(\frac{\partial F_2}{\partial X}\right)$ are defined in Equation 5 through 10 above.

The sensitivities of the mathematical parameters about the operating point X_o, Y_o, Z_o then become

$$S_p^X = p \cdot \left(\frac{\partial X}{\partial p}\right)_o \qquad (X_o=1)$$

$$S_p^y = p \cdot \left(\frac{\partial y}{\partial p}\right)_o \qquad (Y_o=1)$$

with $$\frac{S_p^X}{S_p^X} = G_2 \qquad \text{for all } p \neq G_z.$$

III. The steady-state sensitivities for any physiological parameter p can be expressed in terms of the mathematical parameters as follows:

$$S_p^X = p \left[\frac{\partial A}{\partial p}\left(\frac{\partial X}{\partial A}\right)_o + \frac{\partial B}{\partial p}\left(\frac{\partial X}{\partial B}\right)_o + \frac{\partial C}{\partial p}\left(\frac{\partial X}{\partial C}\right)_o + \frac{\partial D}{\partial p}\left(\frac{\partial X}{\partial D}\right)_o + \frac{\partial n}{\partial p}\left(\frac{\partial X}{\partial n}\right)_o\right]$$

and $$S_p^Y = \frac{S_p^X}{G_2}$$

The components of these equations are defined as follows: The partial derivative of x with respect to A, B, C, D, and n are the same as shown in equation 6 through 10. The partials of A, B, C, D, and n with respect to the physiological parameters $p = V_m$, K_d, P_{50}, P_aO, Q, PV, and k are shown below

for $p = V_m$

$$\frac{\partial A}{\partial V_m} = \frac{G_1 \cdot A}{K_d \cdot P_tO_o}$$

$$\frac{\partial C}{\partial V_m} = \frac{-r \cdot S_aO_o}{\mu \cdot V_m^2}$$

$$\frac{\partial D}{\partial V_m} = \frac{-r(1-S_aO}{\mu \cdot V_m^2}$$

$p = K_d$

$$\frac{\partial A}{\partial K_d} = \frac{-G_1 \cdot V_m \cdot A}{Kd^2 \cdot P_tO_o}$$

$p = P_{50}$

$$\frac{\partial B}{\partial P_{50}} = \frac{G_1}{P_tO}$$

$$\frac{\partial C}{\partial P_{50}} = \frac{-\,k \cdot r \cdot S_a0}{\mu \cdot V_m \cdot P_{50} \cdot \left[1 + \left(\frac{P_o0}{P_{50}}\right)^k\right]}$$

$$\frac{\partial D}{\partial P_{50}} = \frac{-\partial C}{\partial P_{50}}$$

$p = P_a0$

$$\frac{\partial C}{\partial P_a0} = \frac{k \cdot r \cdot S_a0^2}{u \cdot V_m \cdot P_a0} \cdot \left(\frac{P_{50}}{P_a0}\right)^k \cdot$$

$$\frac{\partial D}{\partial P_a0} = \frac{-\partial C}{\partial P_a0}$$

$p = Q$

$$\frac{\partial C}{\partial Q} = \frac{r \cdot S_a0}{Q \cdot \mu \cdot V_m}$$

$$\frac{\partial D}{\partial Q} = \frac{r \cdot (1-S_a0)}{Q - \mu \cdot V_m}$$

$p = PV$

$$\frac{\partial C}{\partial PV} = \frac{-\,C}{PV}$$

$$\frac{\partial D}{\partial PV} = \frac{-D}{PV}$$

p = k

$$\frac{\partial C}{\partial k} = \frac{-r \cdot S_a 0 \cdot (1-S_a 0)}{\mu \cdot V_m} \cdot \log\left(\frac{P_{50}}{P_a 0}\right)$$

$$\frac{\partial D}{\partial k} = \frac{-\partial C}{\partial k}$$

$$\frac{\partial n}{\partial k} = \frac{-1}{k^2}$$

The actual steady-state sensitivity values for each parameter, both mathematical and physiological, for each of the four species are shown in Tables 4 and 5 of the main text of this paper.

APPENDIX B

DERIVATION OF THE EQUATIONS USED TO DETERMINE DYNAMIC SENSITIVITIES

The model can be generally described by the three differential equations,

$$\dot{X} = H_1(X,Z), \quad , \; X(o)=X_o$$

and $$\dot{Y} = H_2(X,Y), \quad , \; Y(o)=Y_o$$

$$\dot{Z} = H_3(Y,Z) \quad , \; Z(o)=Z_o$$

Let p = any mathematical (independent) parameter, the following relations can be defined

$$s_1 = \frac{\partial X}{\partial p} \quad , \quad s_2 = \frac{\partial y}{\partial p} \quad , \text{ and } \quad s_3 = \frac{\partial z}{\partial p} \quad .$$

then it follows that

$$\dot{s}_1 = \frac{\partial H_1}{\partial p} = s_1 \frac{\partial H_1}{\partial x} + s_3 \frac{\partial H_1}{\partial Z} + \left(\frac{\partial H_1}{\partial p}\right)_{x,z} \qquad (1)$$

$$\text{where: } s_1(o) = \begin{cases} 0 & , \quad p \neq X_o \\ 1 & , \quad p = X_o \end{cases}$$

$$\dot{s}_2 = s_1 \frac{\partial H_2}{\partial X} + s_2 \frac{\partial H_2}{\partial y} + \left(\frac{\partial H_2}{\partial p}\right)_{x,y} \qquad (2)$$

$$\text{where: } s_2(o) = \begin{cases} 0 & , \quad p \neq y_o \\ 1 & , \quad p = y_o \end{cases}$$

and

$$\dot{s}_3 = s_2 \frac{\partial H_3}{\partial y} + s_3 \frac{\partial H_3}{\partial z} + \left(\frac{\partial H_3}{\partial p}\right)_{y,z} \qquad (3)$$

$$\text{where: } s_3(o) = \begin{cases} 0 & , \quad p \neq z_o \\ 1 & , \quad p = z_o \end{cases}$$

The derivatives of H_1, H_2, and H_3 can be derived and are shown below.

$$H_1 = K_1 (z-x)$$

$$\frac{\partial H_1}{\partial X} = - K_1$$

$$\frac{\partial H_1}{\partial z} = K_1$$

$$\frac{\partial H_1}{\partial K_1} = z - x$$

$$H_2 = K_2 \, (F_2(x) - y)$$

$$\frac{\partial H_2}{\partial X} = K_2 \, \frac{\partial F_2}{\partial X}$$

$$\frac{\partial H_2}{\partial y} = -K_2$$

$$\frac{\partial H_2}{\partial K_2} = F_2(X) - y$$

$$\frac{\partial H_2}{\partial p} = K_2 \, \frac{\partial F_2(x)}{\partial p} \qquad p \neq K_2$$

$$H_3 = K_3 \, (F_3(y) - z)$$

$$\frac{\partial H_3}{\partial y} = K_3 \, \frac{\partial F_3}{\partial y}$$

$$\frac{\partial H_3}{\partial z} = - K_3$$

$$\frac{\partial H_3}{\partial K_3} = F_3(y) - z$$

$$\frac{\partial H_3}{\partial p} = K_3 \, \frac{\partial F_3}{\partial p} \, , \qquad p \neq K_3$$

The partial derivative required to evaluate the above equations are:

$$\frac{\partial F_2(X)}{\partial X} = \frac{-n \cdot B \cdot (C+D)}{(DX+1)^2} \cdot W(X)^{n-1} \cdot F_2(X)$$

where: $F_2(X) = A \cdot \exp(-BW^n)$ and

$$W = \frac{(CX-1)}{(DX+1)}$$

$$\frac{\partial F_3}{\partial y} = \begin{cases} G_2 y^{(G_2-1)}, & y < 1 \\ G_2/y, & 1 \leq y \leq e^{4/G_2} \\ G_2 \cdot e^{G_2} \cdot e^{-4/G_2} \exp\left(-G_2 \cdot y \cdot e^{-4/G_2}\right), & y > e^{4/G_2} \end{cases}$$

$\frac{\partial F_2}{\partial p}$ = for p = A, B, C, D, n are defined by equations 6-10 in appendix A

$$\frac{\partial F_3}{\partial p} = 0 \quad \text{when } p \neq G_2$$

$$\frac{\partial F_3}{\partial G_2} = K_3 \frac{\partial F_3}{\partial G_2}$$

where $\frac{\partial F_3}{\partial G_2}$ is defined as follows:

$$\frac{\partial F_3}{\partial G_2} = \begin{cases} y^{G_2} \log(y), & y < 1 \\ \log(y), & 1 \le y \le e^{4/G_2} \\ \left[1 - e^{-4/G_2} \cdot y\left(1 + {}^{4/G_2}\right)\right] \cdot e^{G_2} \cdot \exp\left(-G_2 \cdot y \cdot e^{-4/G_2}\right), & y > e^{4/G_2} \end{cases}$$

Substituting the above information into equations 1, 2, and 3 yields the following results:

$$\dot{s}_1 = K_1\left(s_3 - s_1\right) + \begin{cases} 0, & p \neq K_1 \\ \left(z - x\right), & p = K_1 \end{cases} \qquad (4)$$

$$\text{where: } s_1(o) = \begin{cases} 0, & p \neq X_o \\ 1, & p = X_o \end{cases}$$

$$\dot{s}_2 = K_2 \left(s_1 \frac{\partial F_2}{\partial X} - s_2 \right) + \begin{cases} K_2 \dfrac{\partial F_2}{\partial p} , & p \neq K_2 \\ F_2(X) - y , & p = K_2 \end{cases} \qquad (5)$$

$$\text{where: } s_2(o) = \begin{cases} 0 , & p \neq yo \\ 1 , & p = yo \end{cases}$$

$$\dot{s}_3 = K_3 \left(s_2 \frac{\partial F_3}{\partial y} - s_3 \right) + \begin{cases} 0 , & p \neq K_3, G_2 \\ F_3(y) - z , & p = K_3 \\ K_3 \dfrac{\partial F_3(y)}{\partial G_2} , & p = G_2 \end{cases} \qquad (6)$$

$$\text{where: } s_3(o) = \begin{cases} 0 , & p \neq Z_o \\ 1 , & p = Z \end{cases}$$

The dynamic sensitivity coefficients for the mathematical parameters (p = A, B, C, D, n) are then defined as

$$S_p^X = \frac{p}{X} s_1 \qquad (7)$$

$$S_p^y = \frac{p}{y} \cdot s_2 \tag{8}$$

$$S_p^z = \frac{p}{z} \cdot s_3 \tag{9}$$

The dynamic sensitivities in Figures 23-26 of the main text, were obtained by solving Equations 4, 5, and 6 numerically for S_1, S_2, and S_3, then substituting the results into Equations 7, 8, and 9.

The dynamic sensitivities for the physiological parameter shown in Figures 27-29 were obtained in the following manner

$$S_q^V = \frac{q}{V}\left[\frac{\partial A}{\partial q}\left(\frac{\partial V}{\partial A}\right) + \frac{\partial B}{\partial q}\left(\frac{\partial V}{\partial B}\right) + \frac{\partial C}{\partial q}\left(\frac{\partial V}{\partial C}\right) + \frac{\partial D}{\partial Q}\left(\frac{\partial V}{\partial D}\right) + \frac{\partial n}{\partial q}\left(\frac{\partial V}{\partial n}\right)\right] \tag{10}$$

where V = dependent variables x, y, or z,

q = physiological parameters K_d, J_m, P_{50}, P_aO.....

and p = mathematical parameter A, B, C, D, n

Equation 10 can be rewritten as

$$S_q^V = \frac{q}{V}\left[\sum_{p=A}^{n}\left(\frac{\partial p}{\partial q}\right)\cdot\frac{\partial V}{\partial p}\right]$$

where the $\left(\frac{\partial p}{\partial q}\right)'s$ are defined in Appendix A.

and the $\left(\frac{\partial V}{\partial p}\right)'s$ are defined in Appendix A, Equations 6-10.